Astron. Astrophys. 362, 1020–1040 (2000)

ASTRONOMY AND ASTROPHYSICS

Stellar and circumstellar activity in the Be star EW Lacertae from the 1993 multi-site campaign

M. Floquet[1], A.M. Hubert[1], R. Hirata[2], D. McDavid[3,4], J. Zorec[5], D. Gies[6], M. Hahula[6], E. Janot-Pacheco[7,1], E. Kambe[8,9], N.V. Leister[7], S. Štefl[10], A. Tarasov[11], and C. Neiner[1]

[1] Dasgal, UMR 8633 du CNRS, Observatoire de Meudon, 92195 Meudon, France
[2] Department of Astronomy, Kyoto University, Kyoto 606-01, Japan
[3] Limber Observatory, Timber Creek Road, P.O. Box 63599, Pipe Creek, TX 78063-3599, USA
[4] Guest Observer, McDonald Observatory, The University of Texas at Austin, USA
[5] Institut d'Astrophysique, 98bis Boulevard Arago, 75014 Paris, France
[6] Center for High Angular Resolution Astronomy and Department of Physics and Astronomy, Georgia State University, Atlanta, GA 30303-3083, USA
[7] Instituto Astronomico e Geofisico, Universidade de São Paulo, Caixa Postal 3386, 01060-970 São Paulo, Brazil
[8] Department of Geoscience, National Defense Academy, Yokosuka, Kanagawa 239-8686, Japan
[9] Observer at the Dominion Astronomical Observatory (Canada) during the campaign
[10] Astronomical Institute, Academy of Sciences, 251 65 Ondřejov, Czech Republic
[11] Crimean Astrophysical Observatory, Nauchny, Crimea, 334413, Ukraine

Received 4 February 2000 / Accepted 19 July 2000

Abstract. A multi-site, multi-technique campaign on the Be star EW Lac was held for about 9 days in August-September 1993. We present results of the analysis of visual, high S/N spectroscopic data (He I 6678 Å and Hα). Search for short-term variability was carried out on He I 6678 (line profiles, radial velocity (RV), equivalent width (EW), full width at half-maximum (FWHM) on the absorption part of the line profile and on violet (V) and red (R) emission peaks) and on Hα emission line (line profiles, EW, V, R and V/R ratio). The presence of multi-periodicity is confirmed and we detected the frequencies found in 1989 by Floquet et al. (1992) during a 8-day mono-site campaign. Possible non-radial pulsation solutions for the main frequencies detected are $\ell \approx 2$–3, $|m| \approx 2$–3. We found evidence on the He I 6678 line of episodic matter outflows through the presence of relatively broad, variable absorption line-profile variations. At least one sharp absorption feature was also observed slowly crossing the stellar disc. It is attributed to a blob of matter temporarily orbiting the star. A brief account is given of broad-band polarimetric observations, performed over 6 nights. A correlation is found between the variation in intrinsic polarization level in the B-band and He I 6678 Å strength. Finally, we present a simple model that reproduces rather well the additional "pseudo-photosphere" contribution in 1993 as opposed to 1989.

Key words: stars: circumstellar matter – stars: emission-line, Be – stars: oscillations – stars: individual: EW Lac – stars: variables: general

Send offprint requests to: M. Floquet (michele.floquet@obspm.fr)

1. Introduction

The physical conditions giving rise to the so-called "Be phenomenon" that is, to the presence of a circumstellar envelope around some OB stars are still unknown in spite of considerable efforts by the international community in recent years. These stars also show light and line-profile variations with time scales ranging from minutes to years. In fact, three main time scales can be distinguished schematically:

i) short-term variability (from minutes to tens of hours) due to local photospheric and sub-photospheric changes in temperature, velocity and density, possibly related to non-radial pulsations (nrp), to local magnetic fields which still remain to be detected, and to other unidentified processes.
ii) medium-term variability (weeks, months) mainly detected in early Be stars characterized by short-lived and/or long-lived light outbursts somewhat analogous to "flares". Hipparcos photometry has allowed the detection of long-lived outbursts with a gradual brightness increase over about 100 days, followed by a rather slow ($\geq$ 400 days) relaxation phase (Hubert & Floquet 1998). Outbursts in emission lines have also been observed. In the case of μ Cen, monitored each year for several months, a pattern of short-lived outburst cycles associated to a nrp beat phenomenon was derived by Rivinius et al. (1998a).
iii) long-term variability (years, tens of years) observed in both light and circumstellar lines, which is the consequence of global changes in physical and geometrical parameters of the envelope, induced by episodic mass loss enhancements. Several models (propagation of density waves, successively ejected layers with different density and progressive pile-up, partial infall of matter) are competing to explain the

observations. The evidence is increasing, however, that the above processes are present with different relative intensity in individual stars.

Multiperiodicity has been detected mainly in line profile variations (lpv), and there has been continuous progress in spectroscopic modelling codes of pulsationally perturbed stellar photospheres (see Schrijvers et al. 1997; Telting & Schrijvers 1997; Townsend 1997a and b). Low degree g-modes seem to be present in Be stars which would include them among Slow Pulsating B (SPB) variables. A few stars have periods in time scales as short as 1.5–2 hours (η Cen, Janot-Pacheco et al. 1999; 48 Lib, Floquet et al. 1996; 27 CMa, Balona & Rozowsky 1991), which could be attributed to p-modes; these stars would be among "hybrid" stars showing both p- and g- modes (Mathias & Waelkens 1995). However numerous, closely spaced and narrow moving features observed in line profile series are often irregular in intensity and time evolution and have been thought to originate in lower density gas above the photosphere (Gies 1994).

EW Lac (HD 217050, B3 III, V = 5.35, $V \sin i$ = 340 km s^{-1}) is a Be star seen under a high inclination angle. In addition to emission contribution, its spectrum presents typical shell characteristics (narrow absorption features), commonly observed when envelope density is high. Moreover, this star is well known for alternating the quiescent and active shell phases. It has been in an active shell phase since 1976. Multiperiodicity has been detected in both light and photospheric line profiles, so this star has been considered as a good candidate for testing the relation between short-term line profiles and light variation, and for studying circumstellar activity. First, a quasi-periodic (0.7 d) photometric variation was obtained by various observers, among them Lester (1975) who argued that the colour variations could be explained by temperature changes in the stellar photosphere. Second, a period of 0.7228d was deduced from the international photometric campaign in September/October 1983 (Stagg et al. 1988). Three periods were obtained by Pavlovski (1987) from Hvar data in 1982 and Walker data in 1950–51, and by Pavlovski et al. (1993) from a new compilation of the 1983 campaign data and from Yonsei observatory measurements obtained in the same season. All three periods coincide with the periods deduced from spectroscopy: 0.7 d in the V/R ratio of Hγ found from Calar Alto data by Pavlovski & Schneider (1990), and 3 periods (0.80, 0.625 and 0.36 d) in He I 6678 found by Floquet et al. (1992) from OHP data collected in an 8-night run in 1989. As the state of the envelope of EW Lac has varied continuously since 1976, one of the essential points was to confirm the multi-periods and their origin.

The star was observed again in 1993 during of a series of multi-site, multi-wavelength and multi-technique campaigns devoted to bright Be stars (see Hirata 1993). A photometric campaign managed by J. Percy took place simultaneously with spectroscopic observations. Polarimetric data were also obtained both at the Crimean Astrophysical Observatory by A. Tarasov and at McDonald Observatory by D. McDavid. Independent of the optical multi-site campaign, UV spectroscopy was performed on 1993 September 8/9 over 24 hours by G.J. Peters. In this paper we report on the visual spectroscopic campaign which in turn confirms our previous detection of multiperiodicity in photospheric line profiles. Evidence is given of temporarily orbiting clouds around the star and we develop arguments for the existence of a highly variable pseudo-photosphere from simultaneous spectroscopic and polarimetric behaviour. Finally we propose a tentative model of mass loss events which contribute to feed the anisotropic envelope.

2. Stellar parameters revisited

Before moving on to the observational results of EW Lac, we will reconsider stellar parameters such as radius and mass for this rapidly rotating star. It is well known (Collins & Sonneborn 1977) that rapid rotators viewed edge-on are shifted in the HR diagram with respect to non-rotators so that they seem less massive and more evolved than they really are.

The BCD stellar spectrophotometric parameters (λ_{1*} and D_*, respectively, the mean position and value of the stellar Balmer discontinuity) are calibrated in terms of fundamental stellar parameters (Divan & Zorec 1982, Zorec 1986) which obviously correspond to the observed hemisphere-averaged photospheric radiation field. For EW Lac $\lambda_{1*} = 3740$ Å and $D_* = 0.174$ dex, which lead to $M_{\rm V}(\lambda_1, D_*) = -3.18$ mag; $M_{\rm bol}(\lambda_1, D_*) = -4.82$ mag; $\log T_{\rm eff} = 4.253$. From them we obtain a first estimate of stellar radius and mass: $R_*(\lambda_1, D_*) = 8.7 R_\odot$ and $M_*(\lambda_1, D_*) = 7.8 M_\odot$, which imply a critical rotational velocity $V_{\rm c} = 337$ km s^{-1}. As the star is assumed to rotate with an angular velocity as high as $\omega = \Omega/\Omega_{\rm c} = 0.8$–$0.9$ (Slettebak et al. 1992, Moujtahid et al. 1999), its equatorial velocity then would not exceed $V_{\rm e} = 220$–270 km s^{-1}, which nevertheless disagrees with the observed $V \sin i$ = 340 km s^{-1}.

Due to its high $V \sin i$, finding out the true nature of the central object of EW Lac means we have to interpret the observed apparent photospheric parameters by taking into account the effects of stellar rotation on spectra. First of all, we note that the Hipparcos distance d = 337^{+87}_{-57} pc, together with the apparent visual magnitude $V = 5.25$ mag measured at the epoch when total Balmer discontinuity was $D = D_*$ (Moujtahid et al. 1999) and E(B-V) = 0.12 mag, produce a visual absolute magnitude $M_{\rm V}$(Hipp) = $-[2.8^{+0.5}_{-0.4} + \Delta V_{\rm CE}]$ mag, where $\Delta V_{\rm CE} \gtrsim 0$ is the magnitude excess due to the circumstellar envelope. Analysis of EW Lac energy distribution from $\lambda 3500$ to $\lambda 8000$ (Moujtahid & Zorec 2000) shows that $\Delta V_{\rm CE} \simeq +0.2$ mag. Within the parallax uncertainty, this implies that $M_{\rm V}(\lambda_1, D_*) \simeq M_{\rm V}$(Hipp) and thus, that $M_{\rm V}(\lambda_1, D_*)$ is a good approximation of the radiation field in the V-band emitted by the observed rotationally distorted stellar hemisphere. Knowing that as a function of rotational effects $M_{\rm bol}$ varies in the same way as $M_{\rm V}$, we can assume that the emitted bolometric luminosity of EW Lac is reliably given by $L_{\rm obs}(\lambda_1, D_*)/L_\odot = 10^{-0.4[M_{\rm bol}(\lambda_1, D_*) - M^\odot_{\rm bol}]}$. Hence, to relate the observed quantities to those the star would have if it were not rotating, we adopt the following representations:

$$\begin{aligned} L_{\rm obs}(\lambda_1, D_*) &= L_o F_L(\omega, i) \\ D_* &= D_o F_D(\omega, i) \end{aligned} \quad (1)$$

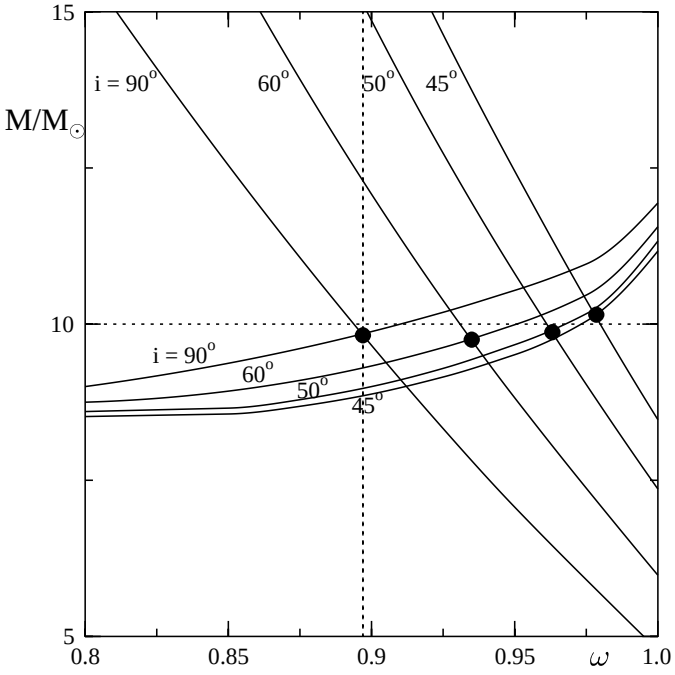

Fig. 1. The mass of EW Lac derived from relations (1) ("vertical urves") and from $V \sin i$ ("horizontal curves"). The dots are the solutions for the given $\omega \gtrsim 0.9$ and the corresponding inclinations i. The vertical dashed line indicates that solutions are possible only for $\omega \gtrsim 0.89$. The horizontal dashed line stands for the mean mass $M_*/M_\odot$ solution

where $F_{\rm L}$ and $F_{\rm D}$ are functions of the angular velocity ratio $\omega = \Omega/\Omega_{\rm c}$ and the inclination angle i, $L_{\rm o}$ and $D_{\rm o}$ are the bolometric luminosity and the Balmer discontinuity of the star without rotation. The functions $F_{\rm L}$ and $F_{\rm D}$ were derived using the Collins & Sonneborn (1977) and Collins et al. (1991) models of rigidly rotating B stars. Inclination averaged $F_{\rm D}$ functions are shown in Zorec & Briot (1997). By parametrizing ω and i we therefore obtain $L_{\rm o}$ and $D_{\rm o}$, from which it follows that therefore $T_{\rm eff} = T_{\rm eff}(D_{\rm o})$ and $R_{\rm o}/R_\odot = (L_{\rm o}/L_\odot)^{1/2}(T_{\rm eff}/T_\odot)^{-2}$ of the non-rotating star. The observed λ_1 parameter of EW Lac implies an apparent luminosity class III. Since we assumed that this luminosity class may be partially due to rotational effects (Slettebak et al. 1980), we adopted only main sequence to subgiant $T_{\rm eff}(D_{\rm o})$ relations. Then, for each (ω, i) we interpolated the corresponding "rest" mass $M_{\rm o} = M_{\rm o}(L_{\rm o}, T_{\rm eff})$ in Maeder & Meynet's (1988) stellar evolutionary tracks. These values are represented in Fig. 1 by the "vertical" curves.

Another estimate of $M_{\rm o}$ as a function of ω and i was obtained by using the observed value of $V \sin i$ and the relation $V \sin i = 340 = V_{\rm c}\omega[R_{\rm e}(\omega)/R_{\rm c}] \sin i \,{\rm km\,s^{-1}}$. The $R_{\rm e}(\omega)$ function used is given in Moujtahid et al. (1999). The masses $M_{\rm o}$ thus obtained are represented in Fig. 1 by the "horizontal" curves. The intersections of both series of curves give, for each possible inclination i and the respective ω, the estimates of the mass we are looking for. The mean value of these determinations is $\overline{M_{\rm o}} = 10.0 \pm 0.3 M_\odot \simeq 1.3 M_*(\lambda_1, D_*)$. Moreover, we note that $M_{\rm o}$ solutions are possible for $0.89 \leq \omega \leq 1.0$ ($i \leq 90°$). In Table 1 we reproduce several stellar parameters obtained as a function of ω: $M_{\rm o}$; $R_{\rm o}$ = "rest" stellar radius; $R_{\rm e}(\omega)$ = equatorial radius distorted by rotation; $V_{\rm e}$ = equatorial rotational velocity and $V_{\rm c}$ = critical equatorial velocity. In Table 1 we see that the new velocities $V_{\rm e}$ obtained are consistent with the observed $V \sin i$.

Table 1. Fundamental parameters of EW Lac as a function of $\omega = \Omega/\Omega_{\rm c}$

ω	$M_{\rm o}/M_\odot$	$R_{\rm o}/R_\odot$	$R_{\rm e}(\omega)/R_\odot$	$V_{\rm e}$ km s^{-1}	$V_{\rm c}$ km s^{-1}
0.90	9.6	6.1	8.1	360	450
0.95	10.0	5.6	7.9	430	480
1.00	10.3	4.9	7.3	530	530

Another straightforward, though less consistent, way of deriving $M_{\rm o}$, uses the relation $R_*(\lambda_1, D) = R_{\rm e}(\omega)$ that leads to an estimate of $R_{\rm o}$ which gives $L_{\rm o}$ combined with $T_{\rm eff}(D_{\rm o})$. The masses $M_{\rm o}$ thus obtained produce curves which are similar to the "vertical" ones shown in Fig. 1. The i-averaged parameters thus obtained are $\overline{M_{\rm o}} = 11.0 \pm 0.7 M_\odot$ and $\overline{R_{\rm o}} = 6.6 \pm 0.5 R_\odot$.

From these estimations we conclude that the central object of EW Lac most probably corresponds to a B1.5-B2 rotating main sequence star, which contrasts with the spectral type B3 III derived from the apparent photospheric parameters.

For this star seen under $i \sim 90°$, we adopt $M_{\rm o}/M_\odot = 9.6 \pm 0.3$, $R_{\rm e}/R_\odot = 8.1 \pm 0.5$ and $V_{\rm e} = 360 \pm 36\,{\rm km\,s^{-1}}$ (an error of 10% is usual for rapidly rotating stars) corresponding to $\omega = 0.90$. The rotational period is estimated as $P_{rot} = 1.14 \pm 0.18$ day ($\Omega_{rot} = 0.88 \pm 0.14$ c/d) and the acceleration of a corotating feature on the stellar equator as $1980 \pm 450\,{\rm km\,s^{-1}}$/d.

It should be kept in mind that the above error bars are obtained adopting Collins & Sonneborn (1977) and Collins et al. (1991) models and Maeder & Meynet (1988) evolutionary tracks.

3. Observational data and reduction

The optical spectroscopic multi-site campaign was carried out at six observatories: Haute Provence (OHP), France, Kitt Peak (KPNO), USA, Dominion (DAO), Canada, Okayama (OKAO), Japan, Crimean (CRAO), Crimea, and Ondřejov (Ond), Czech Republic, from 1993 August 30 to September 8.

The He I 6678 line was monitored at six sites and the Hα line at two sites. Technical observational details are given in Table 2 and the log of observations in Table 3. Bias, flat fields and wavelength calibration exposures produced by Th-Ar lamps were obtained regularly. Reference stars were observed nightly on each site for accurate radial velocity (RV) linking and a better determination of stellar continuum. Luckily, due to good weather conditions at most sites, we obtained a very good temporal coverage in the campaign. The He I line was continuously monitored over two 2.77 and 2.72 day time spans, only interrupted for 7 hours during the 8.6 day campaign.

Table 2. Technical observational conditions in optical spectroscopy

Observatories	OHP	DAO	Kitt Peak	Okayama	Crimea	Ondřejov
Observers	Floquet Hubert	Kambe	Gies Hahula	Hirata	Tarasov	Stefl
Telescope (m)	1.52	1.22	0.9	1.88	2.6	2.0
Dispersion (Å/mm)	7.8	10.1	14.9	8.28	6.0	17
Sp. Resolution	24000	33000	15000	20000	35000	10000
Slit width (Å)	0.28	0.20	0.44	0.33	0.19	Im. Slicer
CCD	Thomson	UBC	Tektronix	RCA	GEC	Reticon
pixel format	2048x1	2048x2048	2048x2048	1024x620	581x385	1872x1
pixel size (μ)	13	15	24	12	10	15
sampling interval (Å)	0.101	0.15	0.166	0.242	0.1055	0.256
binning	1x1	1x3		2x2	1x1	1x1
Spectral coverage (Å)	207	307	340	127	60	390
Observed lines	He I 6678	He I 6678	He I 6678 + Hα	He I 6678	He I 6678	Hα + He I 6678
Number of sp.	84	102	491	47 + 2 Hα	40	14

Table 3. Log of spectroscopic observations

site	date (1993)	hjd - 2449230.0	number of sp	S/N	exp (min)
OHP	Aug 30	0.38–0.64	10	300	30–40
DAO	Aug 31	0.72–0.97	9	$<$200	40
CRAO	Aug 31	1.25–1.59	12	150	40
OHP	Aug 31	1.36–1.64	13	300	30
KPNO	Sept 1	1.66–2.02	165	200–300	2
DAO	Sept 1	1.69–2.02	12	200–300	40
OKAO	Sept 1	1.97–2.24	10	200–300	30–40
OHP	Sept 1	2.34–2.52	7	$>$300	30–45
CRAO	Sept 1	2.41–2.57	6	150	40
KPNO	Sept 2	2.61–3.03	62	200–300	7
DAO	Sept 2	2.67–3.00	12	200–300	40
OHP	Sept 2	3.36–3.65	12	500	30–40
KPNO	Sept 3	3.61–4.02	57	200–300	7
DAO	Sept 3	3.70–3.98	11	200–300	40
OHP	Sept 3	4.31–4.66	15	$>$300	30
CRAO	Sept 3	4.42–4.55	5	150	40
KPNO	Sept 4	4.63 -5.02	61	200–300	7
DAO	Sept 4	4.68–5.02	12	200–300	40
OKAO	Sept 4	5.11–5.28	8	300	25–40
Ond	Sept 4	5.48	1	530	170
CRAO	Sept 4	5.25–5.55	13	200	30–40
OHP	Sept 4	5.35–5.65	11	300–400	45
DAO	Sept 5	5.67–5.93	10	200–300	40
KPNO	Sept 5	5.77–6.02	32	200–300	7
OKAO	Sept 5	5.96–6.25	29	200–300	8–12
CRAO	Sept 5	6.25–6.34	4	100	30–40
Ond	Sept 5	6.53	1	350	99
OHP	Sept 5	6.31–6.66	16	$>$400	30
KPNO	Sept 6	6.63–7.02	57	200–300	7
DAO	Sept 6	6.68–7.03	13	200–300	40
Ond	Sept 7	7.29–7.61	6	470–750	32–60
KPNO	Sept 7	7.62–8.02	57	200–300	7
DAO	Sept 7	7.66–8.01	13	200–300	40
Ond	Sept 7	8.35–8.62	5	400–670	44–67
DAO	Sept 8	8.70–8.98	10	200–300	40
Ond	Sept 9	9.47	1	450	56

For all sites except Crimea and Ondřejov, observations were preliminarily reduced with IRAF[1] by each group of observers. For Crimea and Ondřejov data, reduction was done with local facilities. Kitt Peak spectra were also corrected in the vicinity of Hα for atmospheric contamination. The final reduction steps were done with IRAF by the Meudon group using the one-dimensional spectra provided by observers. Reference regions were carefully selected for satisfactory determination of a pseudo-continuum over about 100 Å around He I 6678. A one piece cubic spline function fitting was applied to these selected regions to determine the continuum level. 778 and 507 spectra were available for the study of He I 6678 and Hα respectively, the S/N ratio varying between 150 and 900. Kitt Peak spectra have the shortest time exposures, especially the first night, due to the combination of gain and simultaneous observation of Hα and He I 6678. We chose not to average the spectra because we preferred to be able to search for high frequencies if they were present. All spectra were corrected for heliocentric velocity; for the He I 6678 study, they were rebinned in the $\lambda\lambda$ 6665–6690 Å wavelength range with the step $\delta\lambda = 0.242$ Å.

Wavelength stability is generally good except for the Crimean spectra which each night show global shifts with respect to other sites. However, these shifts were easily corrected because of overlapping observations on sites. It has to be stressed that good agreement was generally found between different quantities measured on data sets provided by each site when they overlap. However equivalent widths of Ondřejov are smaller by 10% for He I absorption and Hα emission lines obtained at other sites. The small number of spectra obtained at Ondřejov and the lack of overlap in time coverage (only 3 Ondřejov profiles could be compared with others) did not allow us to include them in the search for periodicities in equivalent width and peak intensity; nevertheless they could be used for the study of V/R ratio and

[1] IRAF is distributed by the National Optical Astronomy Observatories, which is operated by the Association of Universities for Research in Astronomy, Inc., under cooperative agreement with the National Science Foundation

RV centroids, these quantities being only weakly affected by discrepancies in equivalent width.

4. General considerations on the behaviour of He I 6678

At first sight the He I 6678 line profiles reveal at least three distinct components (Fig. 2): a broad photospheric-like absorption line profile, a weak central shell feature, and weak blue (V) and red (R) emissions on the outer edges. However the profiles were highly variable over the run, chiefly in their blue wing, and more complex than those previously observed in August-September 1989 at OHP and clearly showing mid-term and short-term timescale variations. This behaviour may be the consequence of a quasi-permanent change in the physical and geometrical parameters of layers above the photosphere as a result of stellar activity at the time of this multi-site campaign.

Differently, the mean profile in August-September 1989 principally displayed a broad symmetrical absorption which could, at first sight, be identified as a rotationally distorted photospheric profile; note that this broad absorption was disturbed in its core by a sharp shell feature due to Fe II 6677 and in outer wings by two very weak, somewhat broad, double emission components.

On profiles obtained from August 30 to September 8, 1993 the weak central shell was not due to Fe II alone, because its radial velocity is not consistent with measurements on other Fe II shell lines observed in the vicinity of Hα. As will be emphasized below, the He I line was strongly disturbed in 1993 by additional broad and narrow absorption features. Moreover the outer weak V and R emissions also varied in width, mean position and intensity. In the following sections it will be stressed that lpv and quantities such as equivalent width (EW) and radial velocity of the centroid of the global absorption component (RV), as well as V and R weak variable emissions, are affected by a mid-term quasi-oscillation that we could not determine accurately, since it is similar to the duration of the observational run. However this variation is fairly well detected in data from all sites and is estimated to be about 9 days, at least.

Since it was not possible to separate the contributions due to the photosphere distorted by stellar rotation and presumably by nrp and by motions in the outer stellar layers and in the circumstellar envelope respectively in each individual profile, we attempted to obtain a qualitative description of the behaviour of both regions. It will be useful in the following to investigate the origin of the detected variations.

4.1. Comparison between 1993 and 1989 data

First, we attempted to fit the broad absorption of the mean He I 6678 profile obtained in September 1989 with a synthetic spectrum of a rotationally distorted photosphere. We adopted T_{eff} = 17900 K and log g = 3.75, values derived from the BCD system for this star. Then we used the code of static NLTE models of stellar atmospheres provided by TLUSTY (Hubeny 1988) and calculated the profile of He I 6678 line with the code SYNSPEC (Hubeny et al. 1994), with $V \sin i$ = 340 km s^{-1}

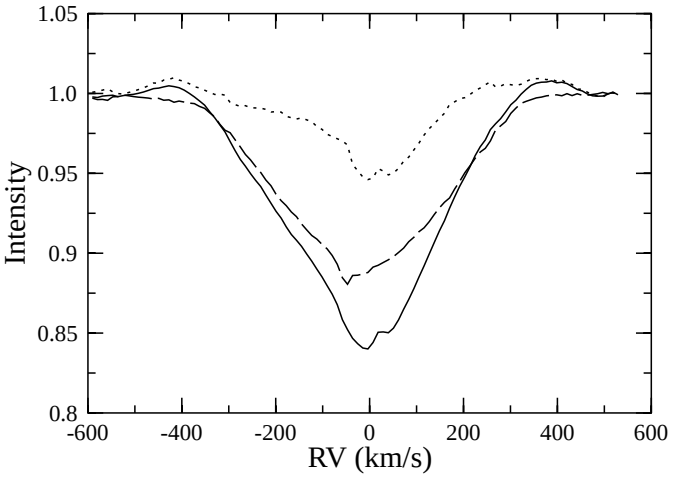

Fig. 2. Mean OHP profiles of the He I line in August-September 1993 (full line), August-September 1989 (dashed line) and quotient 1993/1989 (dotted line)

and v_{th} = 8 km s^{-1}. We observed considerable discrepancy between the observed and computed line profiles of He I 6678 for solar abundance $N_{He}/N_H = 0.1$, the observed equivalent width of this line being always larger by about 30%. Smith et al. (1994) showed that the equivalent width of the He I 6678 line in pulsating B stars and Be stars without strong emission is larger than that of typical dwarfs, while there is good agreement among them for the He I 4922 line. According to Fig. 1 in Smith et al. (1994) the equivalent width of He I 6678 in EW Lac in 1989 is typical of Be stars without strong emission. However, we are not able to derive a reliable He I 6678 photospheric line profile which properly takes into account local effects (temperature, gravity) at the stellar surface due to rapid rotation. Consequently we decided to adopt as a reference the mean profile obtained in 1989, which could be well fitted with a Gaussian curve with an rms of 0.003 measured on the difference between the two curves.

To compare 1993 and 1989 data, Table 4 lists the average value and the maximum deviation of several quantities (equivalent width EW, full width at half maximum FWHM, radial velocity of the centroid RV, central intensity of the core). These quantities were measured on the absorption part of the He I 6678 line profile using IRAF task "Splot". The integration limits were not fixed. Note the lower value of <FWHM> in 1993 as compared to 1989 (325 km s^{-1} compared with 404 km s^{-1}), as well as the amplitude of its mid-term variation ($\pm 13\%$) in 1993. The high EW but low FWHM values in 1993 have incited us to introduce the concept of a pseudo-photosphere, as other authors have already done (see Sect. 7.2). However, the term "pseudo-photosphere" will be used only as a line profile description tool, which in fact is devoid of any preconceived idea as to the line formation region or any line formation model or mechanism. In our description of line profiles, the pseudo-photosphere identifies a spectroscopic characteristic which may actually be produced by a particular stellar atmospheric region, such as an extended and/or moving post photospheric zone. At

Table 4. He I 6678 line profile parameters in 1989 and in 1993

	1989	1993
<EW>	1.00 Å	1.22 Å
δEW/EW	$\pm 7\%$	$\pm 13\%$ (mid-term) $\pm 7\%$ (short-term)
<FWHM>	404 km s^{-1}	325 km s^{-1}
δ(FWHM)/FWHM	$\pm 8\%$	$\pm 13\%$ (mid-term) $\pm 10\%$ (short-term)
<RV (centroid)>	- 13 km/s	- 13 km s^{-1}
Δ(RV)	± 10 km s^{-1}	± 10 km s^{-1} (short-term; amplitude varying)
$< I_{core} >$	0.89	0.84

the line profile description level, it is important to stress that the mixing of short-term and mid-term variations reveals strong activity from August 30 to September 8 1993. As He I 6678 is particularly sensitive to local line formation conditions and to non-LTE effects, small variations in opacity will induce changes in line profiles. We shall see that the mid-term variation of He I affects the whole profile. It was probably due to sporadic expulsion of matter from the star which enlarged the photosphere, giving rise to an effect of lower gravity, and to filling up the inner layers of the envelope as shown in Sect. 4.2.

We examined the quotient of the mean profiles of He I obtained at the same site (OHP) in 1993 and 1989 (Fig. 2). This quotient demonstrates the additional pseudo-photospheric and circumstellar contributions in the 1993 spectra. It is strongly blue-winged, with double V and R emission components, and shows some similarity to Fe II shell lines $\lambda\lambda$ 6456 and 6516 present in the region of Hα.

The Fe II lines are slightly blue-winged and have $RV_{shell} = +10$ km s^{-1}. They are also flanked by weak V and R emission components, centered at -132 and +144 km s^{-1} respectively, and possibly oscillating in intensity, with their V/R ratio always >1; extreme emission wings extend to about ± 300 km s^{-1}.

4.2. The complex variable pseudo-photosphere in 1993

To display the pseudo-photosphere and the circumstellar contribution, quite clearly present in the 1993 data, we divided each individual profile by the 1989 Gaussian fit. The same procedure was also applied to each nightly mean profile from each site to reveal the behaviour of the circumstellar contribution over the run more clearly. This procedure is valid because the mid-term variations in He I 6678 which are induced by changes in physical and geometrical parameters in the pseudo-photosphere/CS inner layers are about 2.5% of the stellar continuum, whereas the expected distortions produced in line profiles by low degree modes of nrp are only about 0.5% (Townsend 1997a).

The resulting daily quotients underscore a complex composite absorption, highly variable in its blue part and flanked by weak outer V and R emissions as seen in Fig. 3 which displays the 9-day gradual fading of a broad component. This very complex absorption can be understood not as a typical profile produced only by an outward moving extended atmosphere, but as the result of the superposition of different contributions (see Fig. 4). Though the composite profiles cannot be resolved unambiguously into different components originating from well-identified regions above the photosphere, an attempt was made to interpret the complex profiles as due to a broad pseudo-photospheric profile, several narrow absorptions super-

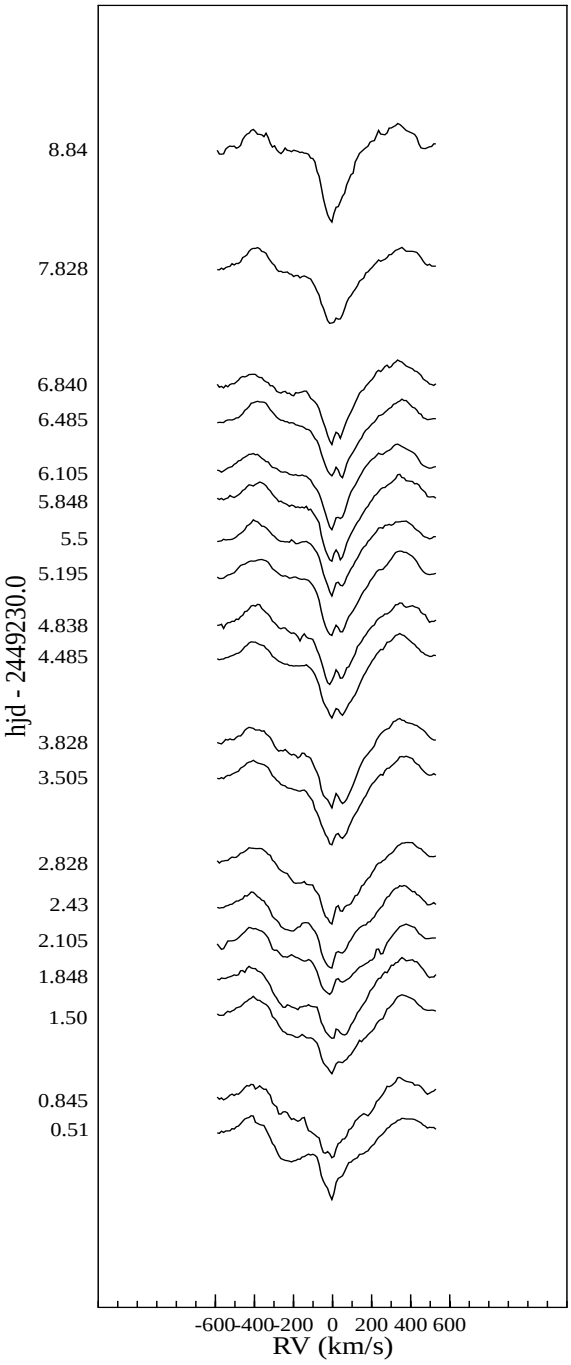

Fig. 3. Temporal evolution of quotients of nightly mean profiles obtained in August-September 1993 (after division by the Gaussian fit of 1989 mean profile) in OHP, OKAO, KPNO and DAO data (the last two are averaged). The mean intensity of the center absorption is 0.05 units of the continuum.

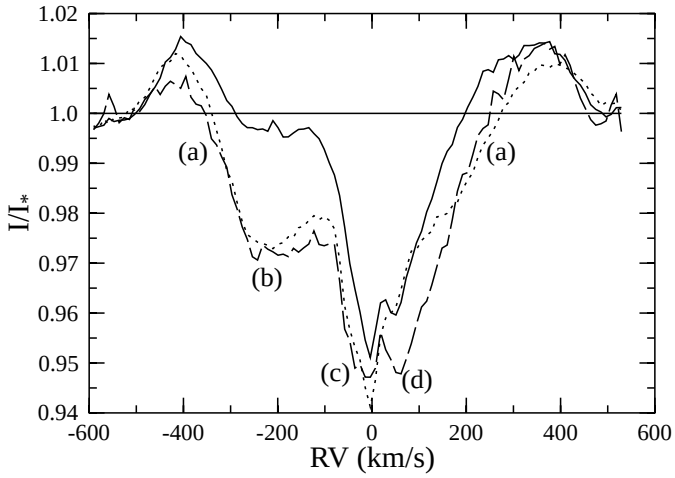

Fig. 4. Examples of quotients of nightly mean profiles obtained in August-September 1993 (after division by the Gaussian fit of 1989 mean profile); dotted line: OHP, hjd 2449230; dashed line: KPNO, hjd 2449231; solid line: OHP, hjd 2449235

imposed on the former, and to weak V and R outer emissions. Under the assumption just made about the structure of the composite profiles, the following components could be identified (see Fig. 4):

- a broad variable absorption (a) whose strength and full width decrease over the run. Its central position determined by the middle of the absorption at the continuum level is blue-shifted towards -50 ± 10 km s^{-1}, i.e. -37 km s^{-1} with respect to the stellar radial velocity ($RV_{star} = -13$ km s^{-1}). This component, which we call pseudo-photosphere, is thought to be due to material ejected prior to the beginning of our run, and its opacity decreases as it expands.
- a narrower blue absorption (b) centered around -200 km s^{-1}, rather stable in position but highly variable in intensity (Fig. 5c). This feature is hardly seen in the second part of the run. This blue component weakened and faded out during the run, in parallel with the broad component (a) suggesting a possible physical connection between them. We shall see in Sect. 7.4 that components (a) and (b) can be understood as manifestations of the same expanding region (ring). On OHP spectra, which in our sample have the highest S/N ratios, several discrete components were detected at the level of the blue absorption (b). They moved redward and were not regularly spaced but had spacings $\Delta t \leq 0.1$ d and a mean apparent acceleration of about 900 km s^{-1}/d (Fig. 6). Their presence in the red part of the component (a) cannot be ruled out.
- two rather strong and narrow absorption components (c) and (d) in a fairly stable position at -13 km s^{-1}, i.e. the stellar radial velocity, and +50 km s^{-1} respectively. The residual intensity at the level of the first component remains constant over the run, the same being true for the second component over 6 days, essentially from HJD 2449231.5 to HJD 2449237.8. Hence it appears that both narrow components increased in intensity over the run while the broad pseudo-photospheric component decreased. We could not resolve each component to determine its FWHM in order to investigate the location of its formation region. At the end of the run, the FWHM of (c) and (d) together is about 200 km s^{-1}, which provides an upper limit to the circular velocity. Component (c) (RV = -13 km s^{-1}) is better defined and could be the result of mass transfer from thequasi-photosphere to the envelope. Component (d) could be associated with infall of a fraction of the ejected material. Both features form the core of the complex CS component.
- two weak V and R emission peaks whose velocity separation decreased over the run from 800 to 720 km s^{-1} (Fig. 5e). The radial velocity of the red peak slightly decreases from 380 to 320 km s^{-1} while the violet peak is roughly stable at around -400 km s^{-1}. We note a gradual shift of the inner edge of the R component (from about +300 to +200 km s^{-1}) and to a lesser degree of the V component (from about -350 to -280 km s^{-1}) towards the center of the line. We shall see that such behaviour is consistent with a detached near-Keplerian ring progressively expanding from the stellar disc.

While the daily behaviour of composite features formed in the pseudo-photosphere can be described simply, this is not possible for the individual profiles which are strongly affected by short-term variations induced by local changes in the stellar disc (nrp and/or inhomogeneities). However, the rapid variability in the strength of blue-shifted absorption near -200 km s^{-1} correlates rather well with the amplitude of short-term variability in the radial velocity of the line centroid at hjd 2449232 and 2449237.8. Moreover, some individual composite circumstellar profiles at both OHP and KPNO show near -150 km s^{-1} a sharp, discrete and short-lived emission which disturbs the slow blue motion of the broad absorption (a) on hourly time-scales. It could be produced by shocks due to ejecta colliding with each other and/or with the circumstellar medium, as well as to the interaction of a supersonic stellar wind with the discrete ejecta.

5. Time series analyses (TSA)

First, it should be emphasized that a period search was done, although the complex profile of He I 6678 includes various types of variation. Indeed, one of the main goals of this study was the confirmation of frequencies detected in 1989 data (Floquet et al. 1992). The main typical quantities of He I 6678 and Hα were investigated first, such as EW, FWHM, the centroid velocity of He I 6678 absorption (RV), the maximal intensity and equivalent width of weak variable V and R emissions flanked on outer edges of the line, along with EW and maximal intensity of V and R components of Hα double emission line. Line profile variability (lpv) analysis was also performed at each resolution element across the He I 6678 line and Hα line profiles. Investigation of multi-periodicity in main quoted variable quantities and in lpv was done using the same methods as in Hubert et al. (1997). Results deduced from 1989 analyses are compared with 1993 data (see Table 5).

Fourier analysis and CLEAN algorithm (method 1) were applied to the measured quantities and to time-series of spectra in

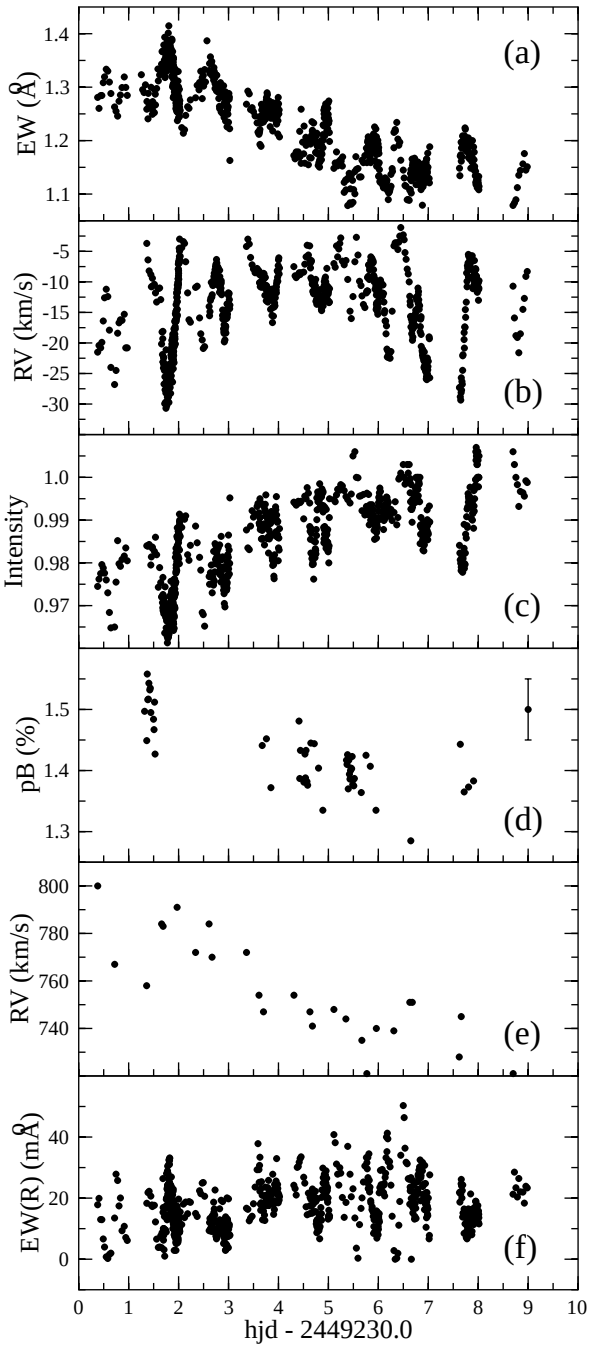

Fig. 5a–f. Temporal variability observed in He I 6678 line. **a**: Equivalent width; **b**: Radial velocity of the line centroid; **c**: Residual intensity of the blue absorption located at -200 km s^{-1} displayed on quotients 1993/1989 gaussian fit (component (b)); **d**: intrinsic B polarization; **e**: Daily radial velocity difference between V and R emission components; **f**: Equivalent width of R emission component

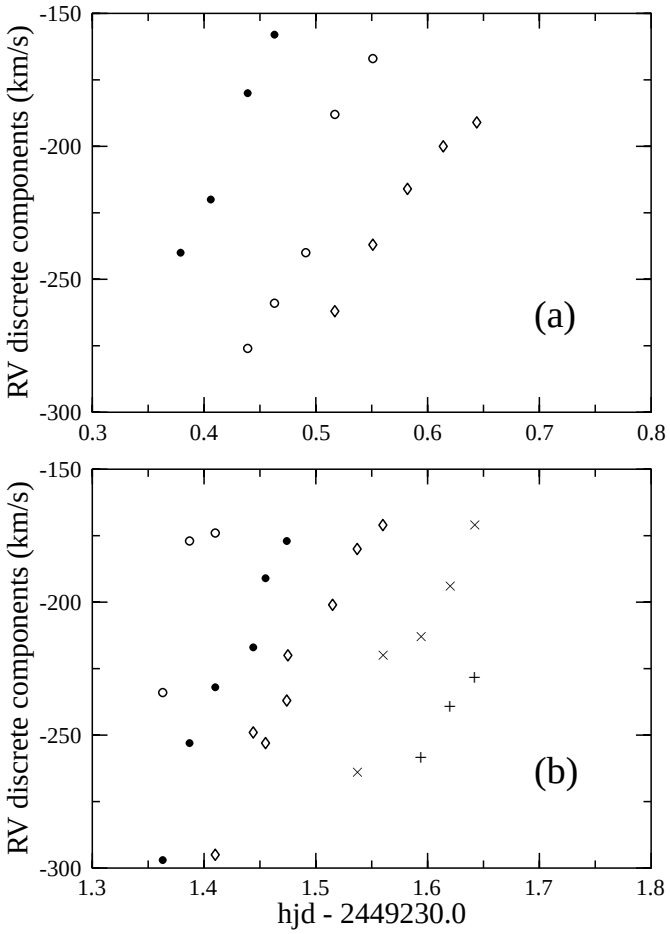

Fig. 6a and b. Radial velocities of discrete components observed near -200 km s^{-1} on OHP quotients 1993/1989 gaussian fit. **a**: on HJD 2449230; **b**: on HJD 2449231

a similar manner to that introduced by Gies and Kullavanijaya (1988). The least-squares sinusoidal fitting (method 2) with the AIC criterion (Kambe et al. 1993 and references therein) was also used in the analysis of lpv. In both methods, weighting by the signal to noise ratio was introduced in the calculation of averaged data. The duration of the observing run was 8.6 days in 1993 and 6.3 days in 1989 and the corresponding frequency resolution (i.e. ν_{min}) was 0.12 and 0.16 c/d respectively. Periods shorter than 0.11 day ($\nu_{max} = 9$ c/d), which corresponds to four times the most frequent exposure time, could not be detected. Mathematical tests were done concerning the value of the frequency over-sampling factor and the best results were obtained for $\nu_{min}/100$. For this value small amplitude frequencies are better recovered. Other tests were done by introducing white noise on a sinusoidal signal with an amplitude varying with wavelength. It was found that the TF+CLEAN method gives correct restoration of frequency values, but the phase determination across the line profile is more accurate with the least-squares sinusoidal fitting method. He I 6678 profiles were scanned every 0.242 Å between 6665 and 6690 Å for time-series analyses.

5.1. He I 6678 line

5.1.1. EW, FWHM and RV variations

The initial profiles normalized to the stellar continuum were used for this investigation.

Equivalent width and FWHM. As indicated above, EW and FWHM were measured in the absorption part of the profiles and did not include blue (V) and red (R) emissions. Due to contamination by these weak emissions, the equivalent width of the absorption is slightly underestimated. The general behaviour of this quantity is seen in Fig. 5a. A relatively large variation, with δEW/EW = $\pm 13\%$, is nicely detected over the observational run on a time-scale of about 9–10 days. From Figs. 3, 4 and 5a it can be concluded that the gradual decrease in EW comes mainly from the vanishing of its broad component (a). Short-term variations are clearly superimposed on the longer one with a semi-amplitude which goes up to 7%. Main frequencies detected in the EW variations are 1.20, 1.51 and 0.89 c/d. Periodograms of EW, RV, V and R emission peaks are given in Fig. 7. This figure also displays the window function.

The central depth of the line is weakly variable around the mean value 0.16 and is deeper than in 1989. Nevertheless this quantity is affected by narrow absorption features (shell contribution) and thus could not be analyzed.

The FWHM parameter was determined with the help of a Gaussian fit to the individual profiles. FWHM variation is dominated by the 9–10 day variability. Its semi-amplitude is 13% over the run and 10% on short-time scales. A 1.20 c/d frequency is detected with method 2 but method 1 gives 2.20 c/d. FWHM and EW are nicely correlated for each data set (site) (Fig. 8). FWHM and EW decrease as R emission increases in the first half of the run (Fig. 5a and f). Moreover, at the beginning of the run they are influenced by broad additional "pseudo-photospheric" absorption (see Sect. 4.2) which was strong from August 30 to September 2, and decreased afterwards. At the end of the run this broad additional absorption was very weak. Conversely, the blended absorptions at -13 and +50 km s^{-1} were strong and narrow and their increase drastically modified the shape and the FWHM of the profiles, as their equivalent width decreased to a lower value close to that of 1989.

Radial velocity. The radial velocity (RV) of the He I line centroid was also measured in the absorption part of the initial profile. The general behaviour of RV can be seen in Fig. 5b. It is clear that rapid variations exhibit a beat phenomenon superimposed on the 9–10 day variation. Radial velocities range between -31 km s^{-1} and -3 km s^{-1}. Frequencies of 1.55 and 1.37 c/d are detected without ambiguity (see Fig. 7c). It is thought that the contribution of weak V and R emission components has no influence on the determination of the line centroid, as frequencies detected in RV variations are also derived from lpv. Indeed, the emission contribution of each component represents only 0.10 to 0.15% of EW.

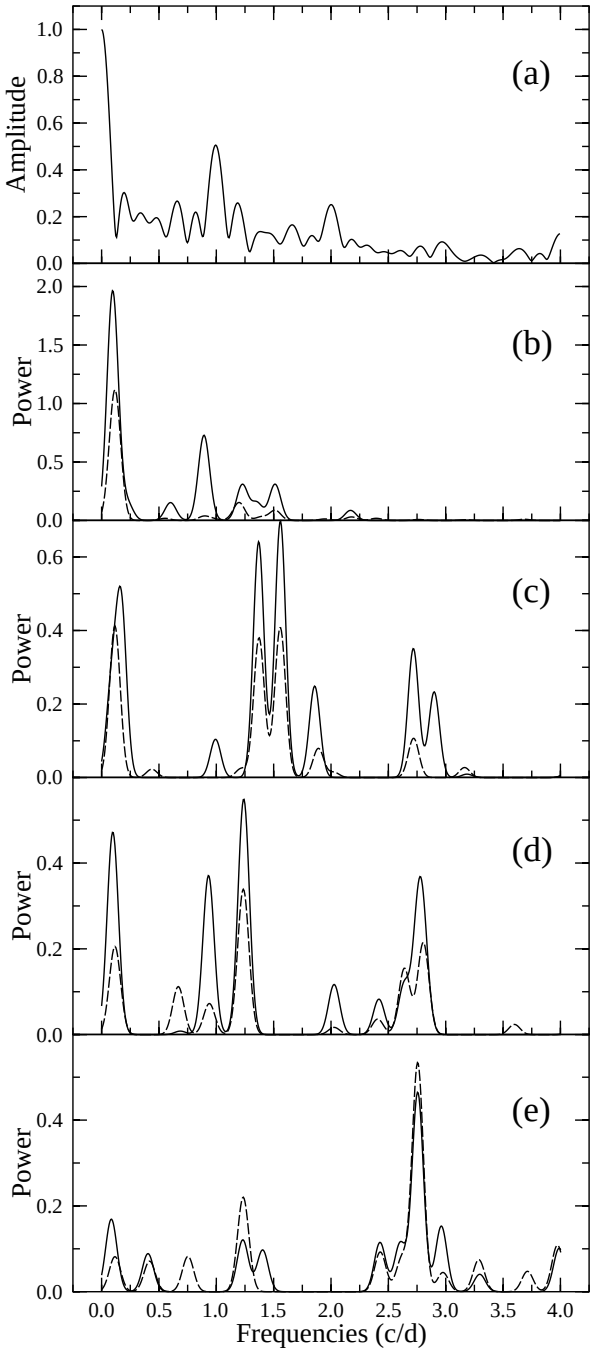

Fig. 7a–e. Periodograms obtained for He I 6678 with Clean (full line) and Least Squares (dashed line) methods. **a**: Window function; **b**: Equivalent width; **c**: Radial velocity; **d**: V emission peak intensity; **e**: R emission peak intensity

5.1.2. V and R emissions

Red emission (R) is essentially always present in the He I profiles, and is variable in intensity, with maxima close to 1.015 ± 0.005; it remains generally stronger than violet emission (V), a which is more difficult to measure due to the strong variability of the blue wing of the photospheric line when the absorption wing reaches -420 km s^{-1}. The daily difference in radial velocities between the V and R peaks decreases over the run (Fig. 5e). The V emission peak is more stable in radial velocity than the R one and lies around -400 km s^{-1} which is greater than $V \sin i = 340$ km s^{-1}, a value adopted by Floquet et al. (1992) for EW Lac. To investigate the importance and the variability of these emissions we measured the maximal intensity of each

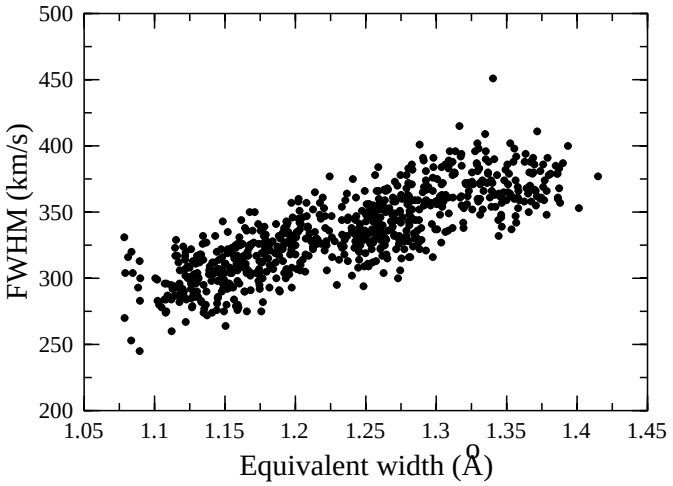

Fig. 8. Correlation between EW and FWHM for He I 6678 in August-September 1993

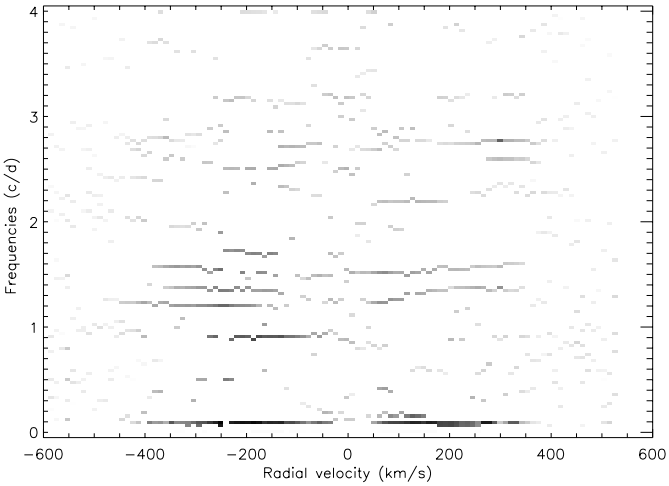

Fig. 9. Clean periodogram obtained from 1993 He I 6678 line profile. Gray scale indicates the power.

peak and their equivalent width measured above the continuum. The variations of equivalent width of the R emission peak are reported in Fig. 5f. In the beginning of the run it shows a slight but gradual increase superimposed on rapid variability. Though the same trend is just slightly detected in the V emission peak, it is found that the sum of the V and R equivalent widths globally increased over the observational run indicating a change over a few days in some physical parameters of the involved layers as in the EW, FWHM and RV of the absorption component. So it can be thought that the behaviour of V and R components is linked to the variation of the additional pseudo-photosphere (components (a) and (b)) and that they are conceivably formed in the same layer.

Periodicities were sought on time-series of each quantity (see Fig. 7d and e). In the R component the dominant frequency is 2.76 c/d. In the V component frequencies 1.24 and 2.77 c/d have been found. In each quantity the amplitude of the signal is strongly modulated over the run by the mid-term oscillation. The 1.22 c/d frequency is mainly detected in the V/R ratio.

To summarize, we find that the V and R emission components generally strengthened, while the FWHM and EW of the photospheric line decreased during the first week of the campaign. Though these quantities are correlated, mid-term variations over 9–10 days detected in FWHM and EW do not result from a combination of V and R emissions with the photospheric profile, but are quite real. Sporadic expulsion of matter from the star would enlarge the extent of the photosphere and could mimic a "photospheric" profile with a lower FWHM value according to computations by Collins et al. (1991); as He I 6678 is particularly sensitive to local formation conditions and to NLTE effects, small opacity variations in outer layers of the photosphere are able to induce detectable changes in line parameters.

5.1.3. Line profile analyses

Intensity variations of He I 6678 were investigated at fixed wavelengths separated by the sampling interval (0.242 Å for 1993 data and 0.101 Å for 1989 data). Frequency analyses were performed in the 0.12–9 c/d frequency range on two sets of data (1993 and 1989) by using two methods described in Sect. 5: Fourier Transform with Clean algorithm (method 1) and the Least Squares sinusoidal fitting with the AIC criterion (method 2). Results are given in Table 5.

We only retained frequencies detected by both methods, powers being somewhat different according to the method used (see Fig. 7). Our reinvestigation of frequencies in 1989 data, with better value of oversampling in the search for frequencies, led to similar values as those contained in Floquet et al. (1992), in which we only used Fast Fourier Transform with Clean algorithm. The 1.60 c/d frequency is highly dominant with both methods; 1.42 c/d is found over the whole profile with method 2 and the 0.42 c/d detected with method 1 is considered to be a one-day alias of 1.42 c/d. Other frequencies with lower power are 2.76, 3.17 and possibly 1.25 c/d detected only with method 1.

For the 1993 data, frequencies obtained with both methods are 0.12, 0.92, 1.22, 1.39, 1.55, 2.76 and 3.20 c/d; most of them were found for the EW (Table 5). With method 2 the AIC criterion decreased steeply for the first 3 detected frequencies (0.12, 1.55 and 1.22 c/d) then varied slightly. Fig. 9 shows the Clean periodogram for 1993.

The 0.12 c/d frequency is due to the mid-term variation whose amplitude dominated throughout the run. It corresponds, in fact, to an upper limit in frequency for this mid-term variation. This time-scale is probably representative of the relaxation time of the outburst which occurred prior to the beginning of the run, since at its end the mid-term variations (EW) were back to the 1989 level.

The 4 frequencies found at 1.55, 1.39, 2.76 and 3.20 c/d deserved careful attention, and were also detected (within the frequency resolution) in the 1989 data. Apart from frequency resolution considerations, the peculiar behaviour of the value of some of these frequencies across the line profile in 1993 data is noteworthy; according to results obtained by method 1, the mean

Table 5. Frequencies (c/d) deduced from the time-series analysis of He I 6678 and Hα profiles in 1993 and He I 6678 in 1989 and common to the two methods. The asterisk indicates that the frequency was obtained only with the Clean method

He I 6678 (1993)							Hα (1993)					He I 6678 (1989)			
lpv	EW	RV	FWHM	V	R	V/R	lpv	EW	V	R	V/R	lpv	residues	EW	RV
0.12	0.12	0.12	0.12	0.10	0.13										0.42
0.92	0.89						0.90	0.91				1.08		1.09	
1.22	1.20		1.20?	1.24	1.23	1.22				2.24				1.23*	
1.39	1.39	1.37					1.42					1.42			
1.55	1.51	1.55					1.60	1.63	1.61	1.65		1.60		1.59*	
2.76				2.77	2.76				2.80		2.73	2.76	2.75		
3.20												3.17			

frequency 1.55 c/d, which extends from -400 to $+380$ km s^{-1}, varies continuously from 1.60 c/d in the photospheric wings where the power is higher to 1.50 c/d towards the core of the line where the signal is lower. Similarly the mean frequency 1.39 c/d, whose extension is $-440, +400$ km s^{-1}, varies from 1.39 c/d in the wings to 1.32 c/d towards the core. This trend depicted from wings to core could explain the lack of coherence in the velocity phase near the center of the profile for both frequencies. This could be due to oscillations produced at different depths or to a superposition of unresolved frequencies. We did not find such behaviour in the 1989 data.

A period variation across the He I 6678 line was also reported for another Be star (ω CMa) by Štefl et al. (1999). These authors found a period value (1.49d) in the far wings of the line profile, well beyond the limit defined by the projected velocity of the stellar limb, slightly greater than the main one (1.37d) found in the photospheric part. A possible origin in CS layers was attributed to the longer period. The behaviour of period variation across the line profile in EW Lac is different from ω CMa. Indeed, both frequencies (1.55 and 1.39 c/d) were found varying continuously from the line center to the $\pm V \sin i$ limit in the outer wings.

The 3.20 c/d appears as a harmonic of the fundamental 1.55 c/d, while the 2.76 c/d is more puzzling, though it could be considered as the first harmonic of the fundamental 1.39 c/d. For this frequency, we should note the strong increase of the power and the abrupt change in the phase velocity at the level of the R emission. This frequency has been detected in IUE spectra obtained on the last day of our campaign on UV photospheric lines using a cross-correlation technique (Peters & Gies 2000).

The 0.92 c/d frequency is mainly detected on the blue part of the profile and extends between -300 and $+100$ km s^{-1}. The corresponding amplitude is higher around -200 km s^{-1}, i.e. in the wavelength region dominated by the blue component (b) (see Sect. 4.2). This frequency falls in the error range for the stellar rotation (see Sect. 2). The 1.22 c/d frequency is weakly present in the red wing of the line, but extends widely towards short wavelengths (-480 km s^{-1}). For these two last frequencies we did not find any coherent phase variation.

nrp investigation. The two frequency groups of 1.55 and 3.20 c/d and of 1.39 and 2.76 c/d (Figs. 10 and 11), which are present in both 1989 and 1993 data, may be associated with nrp modes. To determine ℓ and $|m|$ values we used the method of Telting & Schrijvers (1997) and Schrijvers et al. (1997) applied to the 1993 data. The blue-to-red phase difference for the full wavelength range over which variability is found, $\Delta\Psi$, allows determination of the ℓ value from the fundamental and a rough determination of the $|m|$ value from the first harmonic. More precise values were calculated with the new coefficients given by Schrijvers & Telting (1999) for models taking into account temperature and velocity effects. But as has been shown by Telting & Schrijvers (1997), determination of ℓ and m is not accurate for low degree modes. The errors $\delta\ell$ and δm are estimated to be ± 1 and ± 2 respectively.

The 2.76 c/d frequency can be considered as the first harmonic of 1.39 c/d (case A in Table 6). However, its power distribution does not show the same behaviour over the line profile as the fundamental, as can be expected for the harmonic even in the case of non-adiabaticity effects (Schrijvers & Telting 1999). So we have also considered the possibility that 2.76 c/d is an independent signal (case B in Table 6). Amplitudes for all frequencies, derived from 1989 and 1993 data respectively, are also reported in Table 6. All amplitudes were weaker in 1993, except for the 2.76 c/d signal; the amplitude of the latter was measured outside the red abnormal intensified portion (RV $\sim +300$ km s^{-1}).

As for the 0.92 and 1.22 c/d frequencies found with TSA in 1993 data, we did not find any coherent phase variation over the profile, and we consider that they are not related to nrp.

5.1.4. Evidence of orbiting circumstellar clouds

There is clearly a non-periodic component of the line profile variability which can only be seen on residues formed by subtraction of the run mean profile from individual spectra (Fig. 12). On September 3, a sharp absorption component crosses He I 6678 slower than the other (broader) blue-to-red moving patterns. This sharp feature, which appears first in the OHP spectra, can be followed in the Kitt Peak and DAO spectra; it is seen during 14 hours (HJD 2449233.44–2449234.02) crossing from -200 to +160 km s^{-1}, followed unfortunately by a gap in observations. On September 5, a sharp but weaker feature appears again in OKAO spectra (HJD 2449236.0–2449236.28)

Table 6. Amplitude of common frequencies detected in 1989 and in 1993, and determination of ℓ and m. **Case A**: considering two groups of frequencies as fundamental and first harmonic; **Case B**: 2.76 c/d considered independently

ν (c/d)	Ampl. 1989 (x10^{-3})	Ampl. 1993 (x10^{-3})	$\Delta\Psi/\pi$	Case A ℓ	Case A |m|	Case B ℓ
1.39	8.2	6.9	<2.4	~ 2		
2.76	3.5	4.9	>2.6		~ 2	~ 3
1.55	14	6.6	1.7	~ 2		
3.20	6.3	4.5	~ 3.0		~ 2	

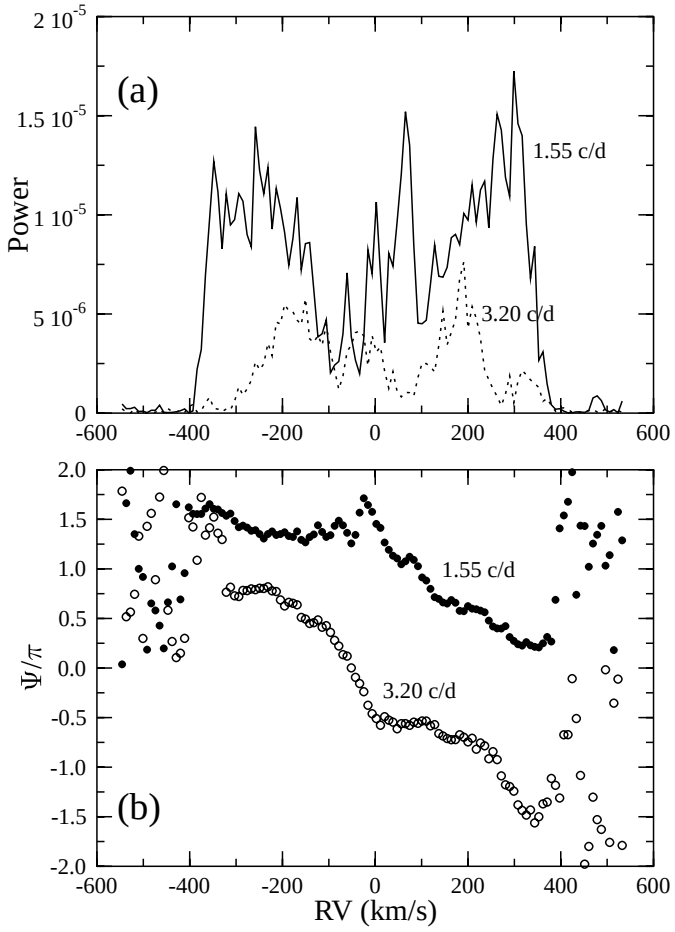

Fig. 10a and b. Power distribution **a** and phase distribution **b** corresponding to the fundamental frequency 1.55 c/d and its first harmonic 3.20 c/d across He I 6678 in August-September 1993.

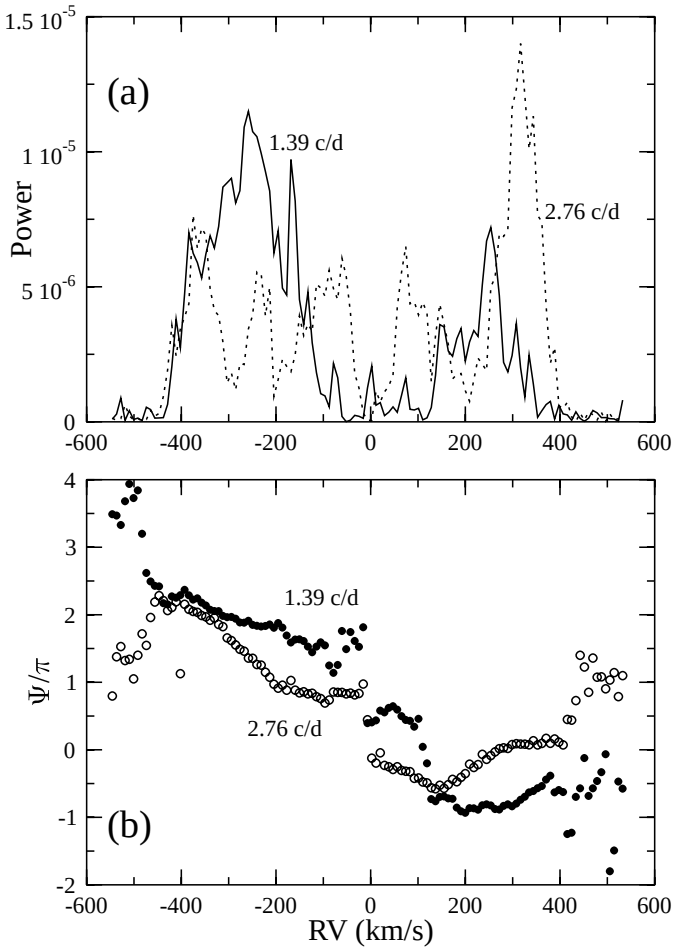

Fig. 11a and b. Power distribution **a** and phase distribution **b** corresponding to the fundamental frequency 1.39 c/d and its first harmonic 2.76 c/d across He I 6678 in August-September 1993.

with about the same transit velocity and during a shorter period (7 hours), observable only near the center of the line (-60 to +40 km s^{-1}). The time span separating the two crossings of the narrow feature at RV $\sim$ 0 km s^{-1} is Δt = 2.4 d.

The acceleration of this feature across the line profile is too low (620 km s^{-1}/d) for a corotating stellar spot. Indeed, at the stellar surface, the acceleration is about 1980 ± 450 km s^{-1}/d (see Sect. 2). These non-periodic features thus originate in the innermost parts of the circumstellar layers.

First, it was assumed that both features are two successive images of the same orbiting cloud. In this picture, if an equatorial plane motion with a circular law is assumed, the circular velocity v_ϕ and the distance r can be reduced from purely observational data from $dv/dt = v_\phi^2/r$ at v = 0 km s^{-1} and P = $2\pi \times r/v_\phi$. Inserting numerical data, dv/dt = 620 km s^{-1}/d and P = 2.4 d, the cloud is found orbiting at about $1.4R_e$; nevertheless its motion is not Keplerian because the derived stellar mass would be too low (3.1 $M_\odot$) compared with the expected mass estimated in Sect. 2 (9.6 $M_\odot$).

Secondly, it was considered that both features are images of different orbiting sub-features having about the same acceleration. In this case if Keplerian motion is assumed, clouds are

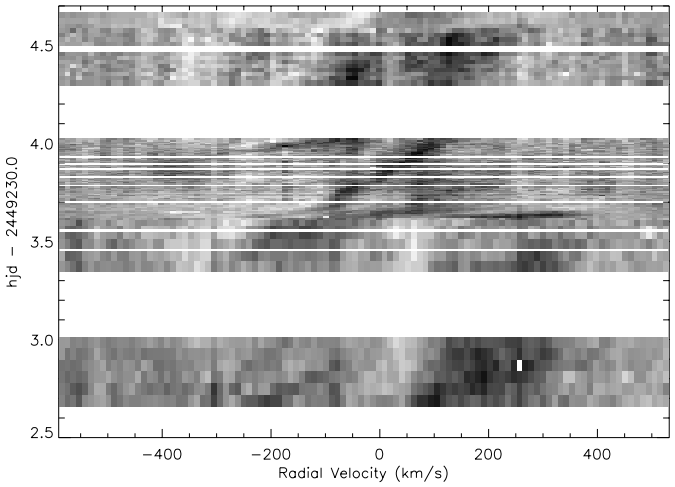

Fig. 12. Gray-scale picture of residues around HJD 2449233.5 showing the transit of an orbiting circumstellar cloud. Observations from DAO, OHP, KPNO and OHP are displayed from bottom to top. As DAO and KPNO observations are simultaneous, we chose to use data from only one site per night.

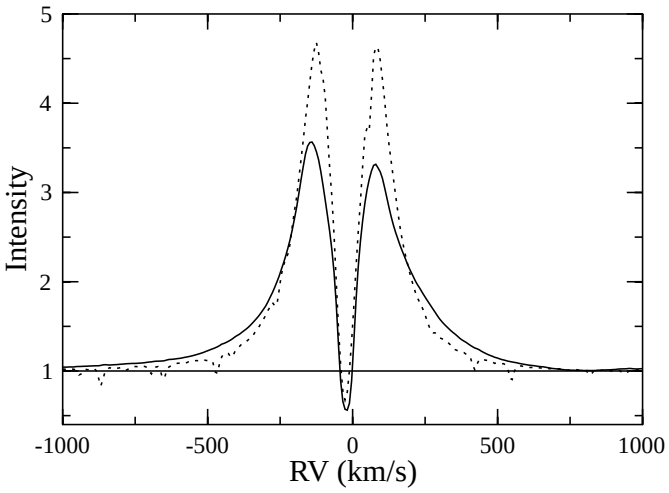

Fig. 13. Mean profile of Hα; full line: 1993 and dashed line: 1989

found orbiting at about $2.4R_e$. As the peak separation of V and R emissions in He I 6678 (which varies from 800 to 720 km s^{-1}) is always larger than $2\,V\,\sin i$, implying the presence of layers which reach Keplerian velocity, it was reasonable to assume that orbiting clouds detected with $a = 620$ km s^{-1}/d have nearly Keplerian motion.

Evidently we have observed the transfer of discrete ejected material to the envelope/disc, resulting from an outflow which occurred just prior to the run. This quantity of material is so small that it induces no important changes in line profile variability; as a matter of fact it is seen when variations in equivalent width and RV of He I are weaker, when the beat phenomenon between 1.39 and 1.55 c/d frequencies has minimal amplitude between HJD 2449233.5–2449235.2.

5.2. Hα line

Hα was intensively monitored from KPNO and also observed from Ondřejov and Okayama observatories. Mean profiles in 1989 and 1993 are given in Fig. 13. In 1993 this strong double peak emission line is slightly asymmetrical with an intensity of 3.5 and a V/R ratio oscillating between 1.02 and 1.16. The overall emission is shifted to the blue with $RV_V = -143$ km s^{-1}, $RV_R = +77$ km s^{-1}, and $RV_{shell} = -23$ km s^{-1}.

In 1989 Hα is stronger, its intensity being 4.85 and V/R $\sim$ 1. The emission line is centered at about RV_{star}, with $RV_V = -112$ km s^{-1}, $RV_R = +90$ km s^{-1} and $RV_{shell} = -16$ km s^{-1}. Note that in 1993 the behaviour of the Hα V/R ratio is the same as for Fe II 6456 with V/R > 1. Nevertheless the shell is red-shifted in Fe II 6456 ($RV = +10$ km s^{-1}) and blue-shifted in Hα ($RV = -23$ km s^{-1}). As a result, the global Hα emission profile in 1993 is not consistent with those generally observed in V/R variables, as it is not as a whole shifted in the same direction as the weaker emission component, in agreement with optically thick line profiles from discs with |m| = 1 perturbation patterns (Okazaki 1996).

No fluctuations in the position of V and R peaks were found in Hα and Fe II 6456.

For the Hα line, we investigated the variation of the intensity of the blue (V) and red (R) emission peaks, the equivalent width (EW), and lpv in the same manner as for He I 6678. In Hα the V emission peak shows a short-term variation superimposed on a monotonic increase (3%), and the R peak shows only short-term variability (Fig. 14a,b). Note that these two quantities are sometimes in phase and sometimes out of phase. Periodograms of EW, V and R, and the corresponding window function are given in Fig. 15.

The V emitting component shows 1.61 and 2.80 c/d oscillations and the R component by 2.24 and 1.65 c/d (see Table 5). The equivalent width of the line is dominated by the 1.63 c/d frequency. It also shows a slight increase (3%) over the run (see Fig. 14c), which correlates with the V peak variation.

TSA applied to the line profiles reveals the presence of common frequencies with He I 6678 (1.60, 1.42 and to a lesser degree 0.90 c/d). These frequencies are detected within ± 400 km s^{-1} limits ($\sim$ He I 6678 velocity range), so we consider that they are linked to subjacent photospheric variability. The amplitude of the signal corresponding to each frequency, after normalization to the intensity of the emission line in each respective scan, remains higher than in He I 6678. At first sight this effect is more important in the center than in the wings; however, it has to be considered with caution and needs to be confirmed. Indeed the uncertainty on the continuum determination was estimated at about 0.7%, which is of the same order as the amplitude of variation observed for He I 6678. Moreover, in the Hα line, extended wings can affect the normalisation procedure and the strong emission amplifies the continuum level effects. The Hα profiles used in this study need a careful correction in the continuum determination, which will be the object of further study. Thus, due to these uncertainties on the continuum determination, we are not able to discriminate between short-term variations due to

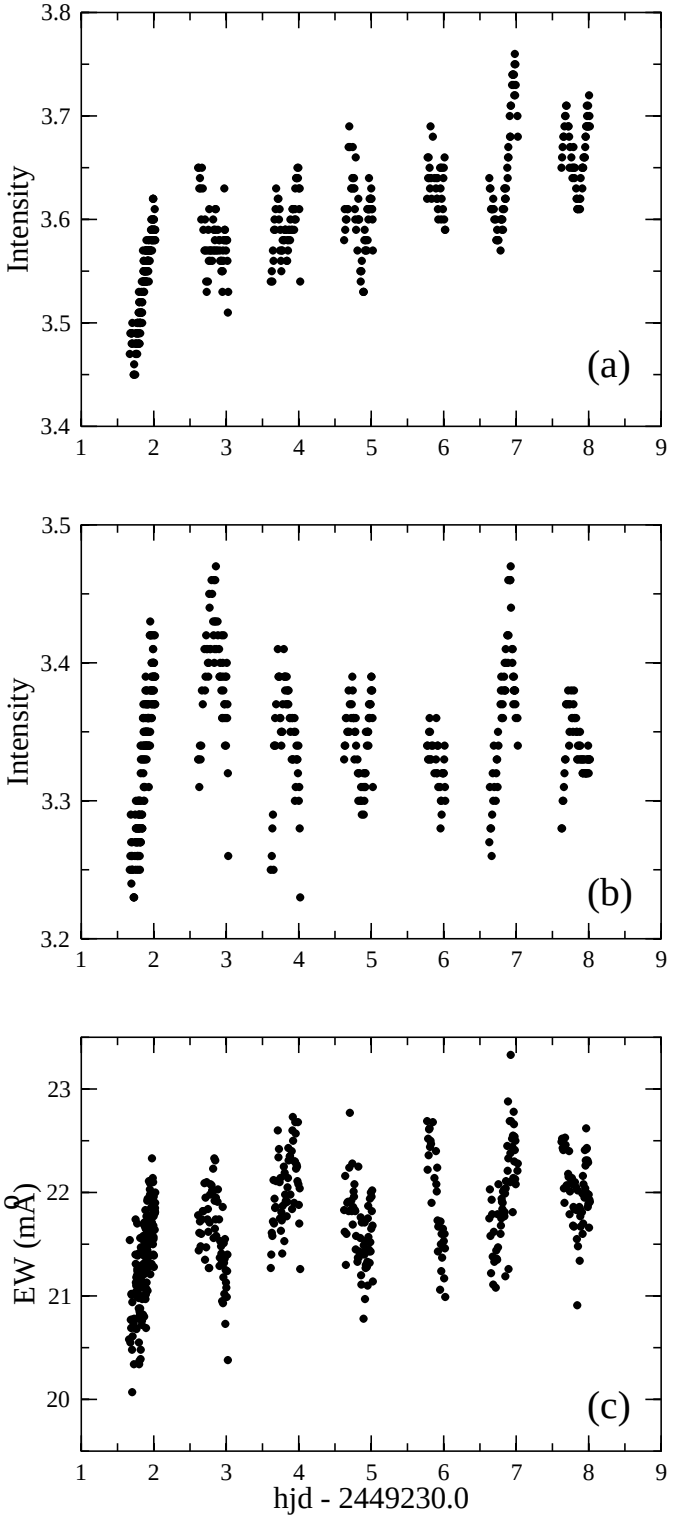

Fig. 14a–c. Variations in Hα line; **a**: V emission peak intensity; **b**: R emission peak intensity; **c**: Equivalent width of the emission line

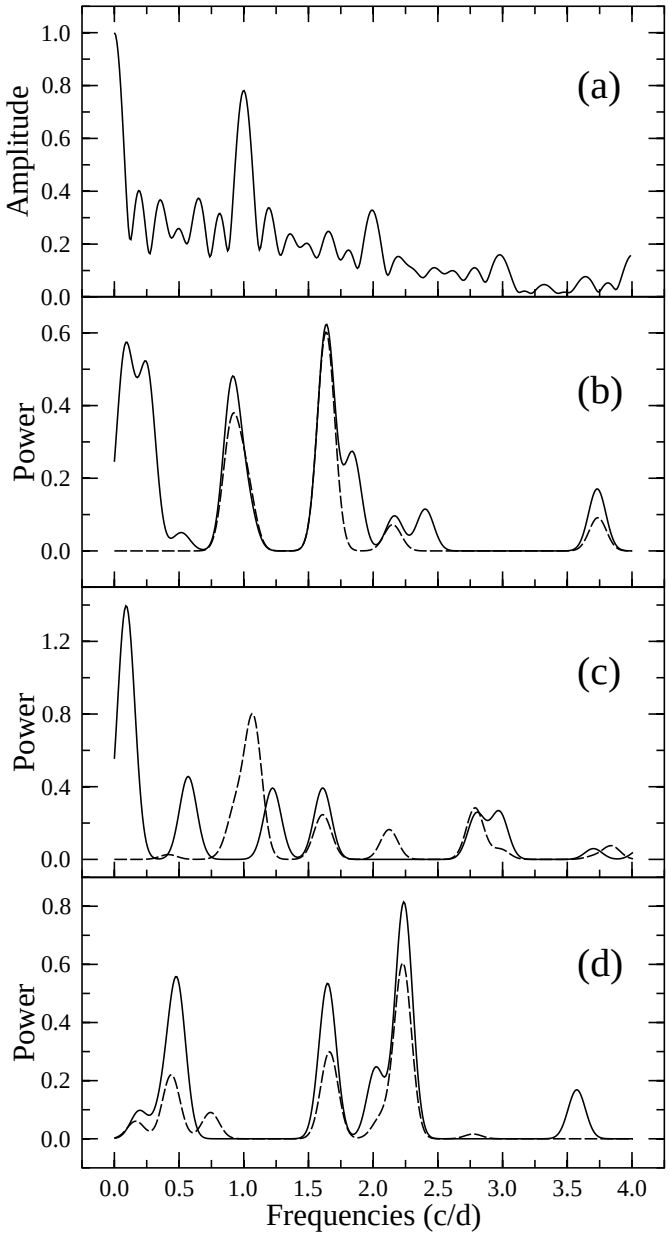

Fig. 15a–d. Periodograms obtained for Hα with Clean (full line) and Least Squares (dashed line) methods. **a**: Window function; **b**: Equivalent width; **c**: V emission peak intensity; **d**: R emission peak intensity

nrp effects on the subjacent photospheric profile and a possible amplification of nrp in inner CS layers. The increase over the run of equivalent width, correlating with V emission peak intensity, can be partially explained by the greater gradual decrease of the pseudo-photospheric component in the blue part of the profile, assuming a similar behaviour in He I and in Hα photospheric line profiles. Nevertheless episodic mass transfer from the star to the envelope should contribute to some enhancement of the line.

The Hα profile in 1993 has a lower intensity but is wider than that of 1989. Such an effect was also observed by Hanuschik et al. (1996) in several stars such as 56 Eri, ω Ori, HR 2284 and o Aqr. The broadening effect in emission line wings is generally attributed to electron scattering according to Castor et al. (1970) and Poeckert & Marlborough (1979). The main difficulty in explaining the Hα line profile variation only by an increase of

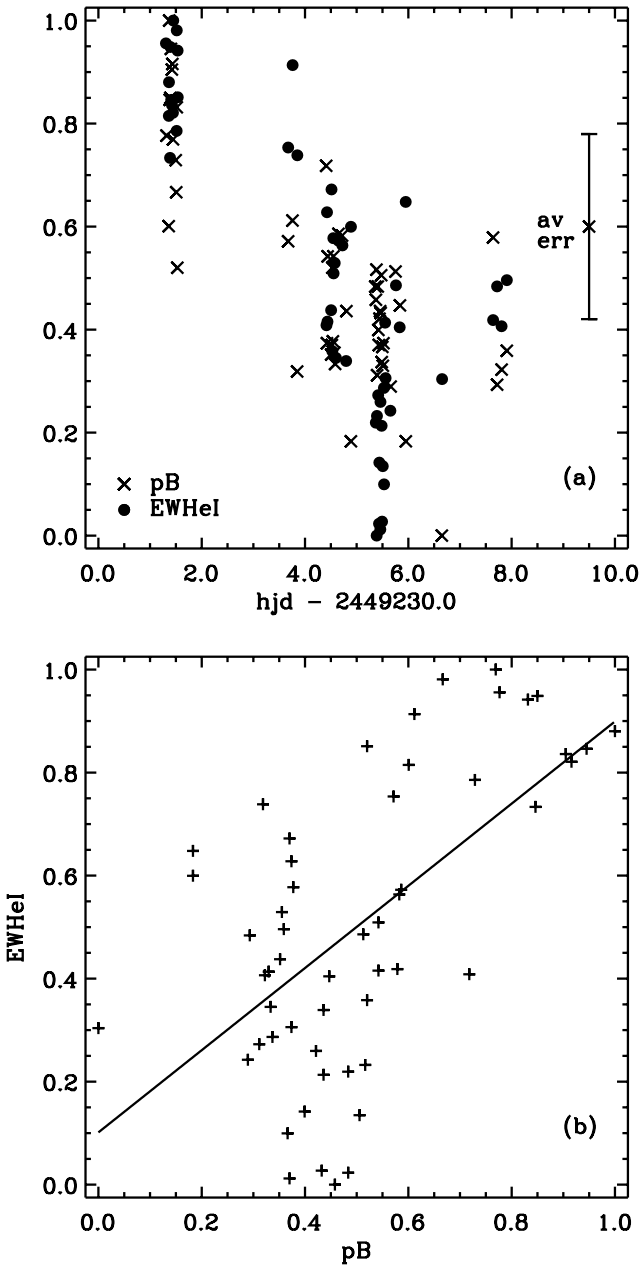

Fig. 16. a: All intrinsic B polarization data points together with the He I 6678 equivalent widths observed at most nearly the same times. **b** Correlation between the B polarization and the He 1 6678 equivalent width. Both quantities were normalized for comparison

scattering effect is that the mean equivalent width changed from EW(1989) = -28Å to EW(1993) = -22Å while it is assumed to be conserved in the redistribution process (Mihalas 1978). It is then possible that other mechanisms involved in the long-term V/R changes also contribute to the line variation.

6. Polarization

Polarimetric data were obtained at the Crimean Observatory in 5 colors (UBVRI) and at McDonald Observatory in a B filter over six nights simultaneously with the spectroscopic campaign. In this paper only results derived from observations in the B filter are reported, after correction for the interstellar component determined by Poeckert et al. (1979). As in the spectroscopy, a rapid variation superimposed on a mid-term one was detected in the degree of polarization (Fig. 5d). The position angle was constant, and no significant periodicities could be found.

A positive correlation of decreasing polarization with decreasing absorption equivalent width of He 1 6678 is suggested by Fig. 5a and c. Fig. 16a shows all B polarization data points together with the individual He 1 6678 equivalent width data points at the most nearly matching times. The average time difference was 0.01 d and the greatest time difference was 0.04 d. Fig. 16b shows graphically the degree of correlation between the two quantities, which were normalized for comparison. The Spearman rank-order correlation coefficient is 0.533. The corresponding value of the complementary error function indicates a probability of 0.003% that the observed correlation would be found if the data were selected at random.

The simultaneous decrease in He 1 6678 equivalent width and B polarization might trace the dissipation of an expanding ring of gas ejected from the star, which would produce a drop in polarization due to the reduction in number density of scattering electrons as the gas expanded. At the same time, the accompanying decrease in opacity of the expanding gas would dilute the polarization by allowing more transmission of unpolarized light directly from the star. Geometrical dilution would also contribute to the polarization decrease as the scattering material moved farther away from the star.

The Spearman rank-order test shows no statistically significant correlation between the B polarization and the equivalent width, V intensity peak, or R intensity peak of the Hα line profile.

7. Discussion

Ground-based photometric campaigns (Stagg et al. 1988), Hvar (Pavlovski et al. 1997) and AAVSO (Percy et al. 1996) surveys, and space data provided by the Hipparcos mission and analyzed in Hubert & Floquet (1998) have given us information on the occurrence of temporary fadings in EW Lac on time-scales of a few days, with δV = δHp = 0.15 mag (Fig. 17a). The shortest time span detected between two fadings from those data is about 60 days. We argue that fadings are related to episodic outflows in this Be star seen nearly equator-on. Results derived from the 1993 multi-site campaign have provided evidence of other signs of episodic outflows, such as broad additional "pseudo-photospheric" absorption slowly expanding, discrete and narrow blue-shifted absorptions, and temporary enhancement of polarized flux. The correlation between EW He I and polarization is unmistakable, but on the other hand, there is little or no direct correlation between polarization and Hα. Our investigation of Fe II $\lambda\lambda$ 6456 and 6516, Hα and He I 6678 seems to show that there is no clear link between the "pseudo-photosphere" and CS layers, even if the latter are fed by transfer of material ejected from the star.

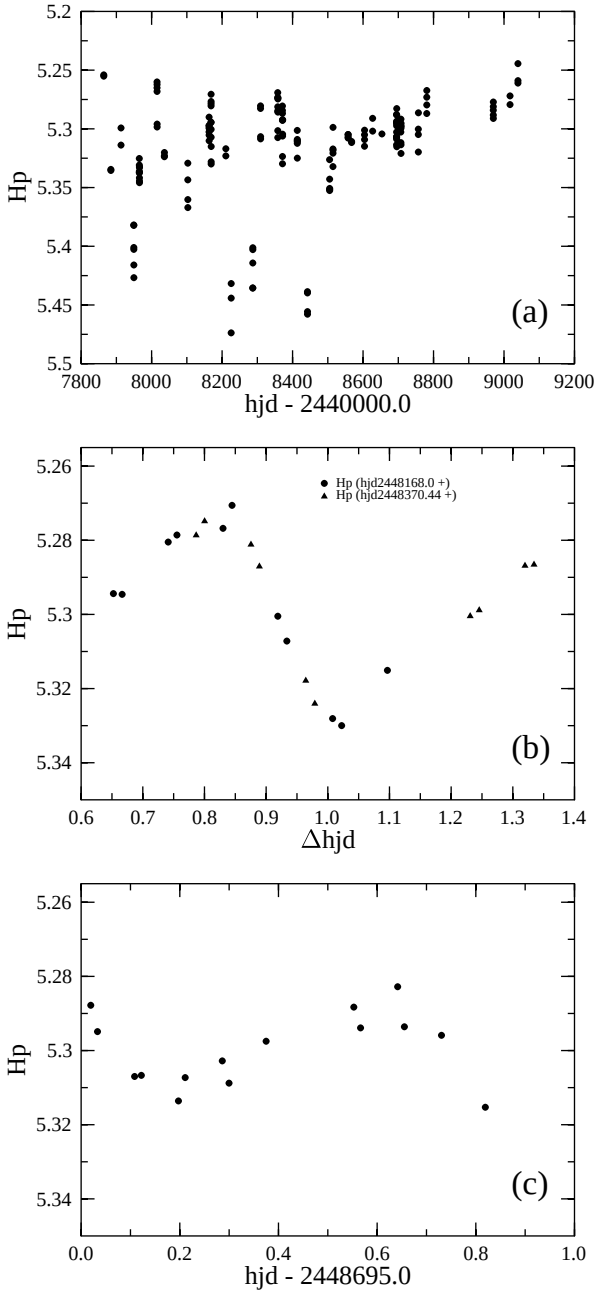

Fig. 17a–c. Hipparcos photometry for EW Lac. **a**: over the whole Hipparcos run; **b**: two continuous series of Hipparcos observations HJD 2448168 and HJD 2448371 put together. These series are shifted in time and also in magnitude (δHp = -0.006 for the observations at HJD 2448371) to put their variations in coincidence; **c**: continuous series of Hipparcos observations at HJD 2448695. Note the difference in amplitude variation between **b** and **c**

Rivinius et al. (1998a and b) have recently shown that outbursts in μ Cen are governed by the zero phase difference and the maximum amplitude sum of two given nrp modes of same ℓ and m. In the case of EW Lac, such a conclusion is premature. Indeed, only two sets of data (August-September 1989 and August-September 1993) limited to the He I 6678 line are available. As shown, this line is particularly sensitive to stellar and circumstellar activity, and our investigation of nrp remains very limited since the stability and the phase coherence of main frequencies could not be sought with good accuracy. Nevertheless it is interesting to note the presence of the same frequencies, within the accuracy limits, in several previous photometric and spectroscopic analyses and in both sets of data of our study (see Table 7). Investigation of short-term variability in several continuous series of Hipparcos data from end-1989 to mid-1993, also supports this conclusion. It has shown evidence of the 0.60 d period (1.67 c/d frequency), with a total amplitude 0.055 mag, near epochs of fadings. Another series in 1992, apparently not disturbed by fadings, has shown a longer period 0.68 d (frequency 1.4 c/d), with a lower total amplitude (0.02 mag) (Figs. 17b and c).

Table 7. Common frequencies detected in EW Lac from different studies

Authors	data	main frequencies (c/d)
Lester 1975	uvby	$\sim$1.39
Stagg et al. 1988	UBV	$\sim$1.39
Pavlovski et al. 1993	UBV	1.27, 1.61, 2.79
Percy et al. 1996	BV	1.56, 1.23
Hubert & Floquet 1998	Hipparcos	1.40, 1.67
Pavlovski & Schneider 1990	V/R Hγ	1.35, 2.9
Peters 1998	IUE EW CIV	1.67
Peters & Gies 2000	IUE, stellar lines	2.86
this study	He I 6678	1.22, 1.39, 1.55, 2.76
	Hα	1.42, 1.60

The amplitude maxima in short-term variability of He I radial velocity over the run in 1993 is observed around HJD 2449231.6-2449232.1 and HJD 2449237.6-2449238.0, which corresponds quite well to the beat of the 1.39 and 1.55 c/d frequencies (cf Fig. 5b and Table 5).

The following discussion will focus on some particularities and interpretation of signals associated with frequencies detected in 1993, and on some physical parameters which can be derived from detected orbiting clouds and from evolution of the behaviour of the He I line profile.

7.1. nrp and rotational modulation

According to Sect. 2, frequencies 1.39, 1.55 and 1.22 c/d are distinct from the rotational frequency ($\Omega_{rot} = 0.88 \pm 0.14$ c/d). Results given in Sect. 5 (Table 6) enable us to assert the presence, in 1989 and 1993, of two groups of frequencies of stellar origin: 1.55–3.20 and 1.39–2.76 c/d. The 1.55 c/d frequency is also the dominant frequency, in the limit of accuracy, detected

in 1989 over the He I 6678 line profile. In terms of nrp this could be associated with a low degree sectoral or tesseral mode. Its power distribution concentrated in the wings indicates for dominating horizontal velocities and favours a g-mode. This frequency is also detected over the Hα emission line. As emission is formed in geometrically extended CS layers going up to several stellar radii, we argue that this frequency concerns the subjacent photosphere and not the extended CS layers which mainly contribute to the Hα emission strength (see Sect. 5.2). Note that Peters (1998) also suspected a similar frequency (P = 0.60: d) in the equivalent width of C IV UV resonance lines from continuous 24-hour monitoring with IUE during the last day of the optical multi-site campaign. So, this frequency is present in the wind and in the photosphere.

The 1.39 c/d frequency is essentially detected in the wings of He I 6678 (see Fig. 11) as opposed to frequencies 1.55, 3.20 c/d and also 2.76 c/d; its power distribution peaks at $\pm 0.71\ V\ \sin i$. However it is stronger in the blue wing and is probably disturbed by the blue absorption component (b) located near -200 km s^{-1}. Its corresponding period 0.72 d has often been reported as the photometric period (Stagg et al. 1988). If the 1.55 and 1.39 c/d frequencies are related to nrp effects on the stellar surface, a strong coupling between them is suggested by the RV centroid behaviour (cf. Fig. 5).

As mentioned above, the 2.76 c/d frequency could first be understood as the first harmonic of 1.39 c/d, except that its behaviour across the line profile is somewhat different (see Fig. 11). Indeed, its power distribution is strongly enhanced at the R emission wing, and its phase velocity breaks off near +150 km s^{-1}. If asymmetry in power distribution is not induced by non-adiabatic temperature effects, it could be indicative of "a wave leakage through the surface and presumably into the wind", according to Townsend (1997a, b). Influence of photospheric variability on the close CS matter has already been detected in another Be star, μ Cen, as reported by Rivinius et al. (1998 a, b). This frequency is also present in UV photospheric lines (Peters & Gies 2000), and could be attributed to an independent nrp mode (see Table 6, case B).

Other frequencies, 0.92 and 1.22 c/d, are mainly detected in the blue wing of He I 6678 and cannot be associated with nrp. The 1.22 c/d frequency could be the result of a beat between 2.76 and 1.55 c/d. A 1.25 c/d frequency is weakly present in 1989 data and appears among frequencies derived by Pavlovski et al. (1997) and by Percy (private communication) from the August/September 1993 photometric campaign. Both frequencies 0.92 and 1.22 c/d are inferred in short-term variations of main quantities and lpv of He I 6678; they are probably linked with outflows modulated by rotation or with a coupling between frequencies presumably associated with nrp and rotation.

It is quite evident that this nrp investigation is only exploratory, as no comparison between computed and observed line profiles could be made. In fact, the He I 6678 profiles obtained in 1993 are so affected by pseudo-photosphere contribution that they are inappropriate for a comparison with modelled photospheric profiles. The stronger argument for nrp put forth in this paper is the evidence of common frequencies in both sets of analyzed data and the fact that some of them are also present in previous spectroscopic and photometric studies (Table 7).

7.2. CS activity versus stellar activity

As it is not easy to find direct links between stellar and circumstellar variability in this complex shell star, we have tried to underscore the results that could shed some light on this point. To begin with, the concept of an extended photosphere/pseudo-photosphere was introduced in the past by several authors. Harmanec (1983) introduced the concept of a pseudo-photosphere by taking into account the inner parts of the envelope which are flattened towards the stellar equator and optically thick in the continuum to explain the observed photometric correlations by an aspect angle. Hirata (1995) assumed the presence of an "extended atmosphere" optically thick even in the optical continuum, in order to explain a drastic change in brightness prior to envelope enhancement (Hα emission) in late active Be stars (Pleione, 88 Her and κ Dra). Similarly, Koubský et al. (1997) argued that the formation of a new Be phase in the late Be type star 4 Her started with the creation of a slightly cooler pseudo-photosphere at the equatorial region which grows into an optically thin extended envelope. EW Lac is a new example of a Be star showing a pseudo-photosphere. However the time scale, as well as the lines sensitive to the effect of the building of a pseudo-photosphere, are probably different in early Be type stars. The common behaviour of the additional broad variable "pseudo-photospheric" component (a) described in Sect. 4.2 and of the V and R outer emission components of He I have to be emphasized. Both are relevant to the same ejected layer: component (a) strength weakens over the 8.6 day run; simultaneously the peak separation of V and R components decreases from 800 to 720 km s^{-1} as R moves from +380 to + 320 km s^{-1}. Qualitatively this can be explained by a ring first rotating closely to the stellar surface at Keplerian velocity, then detaching from the star and slowly expanding over some days during which opacity decreases.

It is possible to think that this ring is formed by repeated discrete outflows of matter that are progressively pushed, since some facts could support this hypothesis. V emission peak minima do not always have the same intensity, and sometimes emission in the blue edge disappears completely (V=1); these pronounced minima occurred more conspicuously at the beginning of the run at intervals of about 1.1 d, corresponding to the frequency 0.92 c/d, and near HJD 2449236 at intervals of about 0.77–0.80 d in agreement with frequency 1.22 c/d. These two frequencies are the most dominant in 1993 data but with unequally distributed power, stronger in the blue wing of He I 6678. Epochs with V=1 could correspond to a dimming of the blue lobe due to an ejected ring associated with the broad component (a), as discrete outflows occur. It is rather interesting to note that the frequency 1.22 c/d, is compatible with the most probable one (1.28 c/d) derived by Percy (private communication) from the 1993 photometric campaign. Is this photometric period due to rotational modulation of some discrete outflows?

7.3. Characteristics of an orbiting circumstellar cloud

Smith & Polidan (1993) showed that a He I 6678 absorption line is formed in rings with column densities at least as high as $N_{2^1P} \sim 8 \times 10^{11}$ He I atoms in the 2^1P level. This is consistent with an optical depth in the center of the line $\tau_o = 7.1 \times 10^{-12}(N_{2^1P}/v_D) \simeq 0.9$ for $T_e \simeq 10^4$ K. We note that our interpretation of the He I 6678 line characteristics demands optical depths $\tau_o \leq 0.5$ (see Sect. 7.4). To derive some physical characteristics of the cloud, which produces the non-periodic sharp absorption in the He I 6678 line, we can think of it as a gaseous spherical blob with radius R_b that crosses over the stellar disc. The residual intensity r_o of the absorption feature that it produces is then given by:

$$r_o = \left(\frac{R_b}{R_*}\right)^2 \left(1 - \frac{S_o}{F_*}\right)\left(1 - e^{-\tau_o}\right) \quad (2)$$

where $S_o = B_o(T_r)$ and $B_o/F_* \simeq 0.40 \pm 0.11$ for excitation temperatures $T_r = 1.0 \pm 0.1 \times 10^4$ K at the distances $1.4 \leq R/R_e \leq 2.4$ derived in Sect. 5.1.4 from kinematic arguments. The relation between T_r and the extent R/R_e comes from Moujtahid et al. (2000). We note that these temperatures are typical for environments which produce "shell" spectra. Hence, assuming a marginal value $\tau_o \simeq 1$ from (Eq. 2) and the measured value $r_o = 0.009 \pm 0.001$, we obtain: $R_b/R_e = 0.16 \pm 0.02$. If the cloud is assumed to have a uniform density and a mean temperature calculated from those derived above, the column density $N_{2^1P}(\mathrm{cm}^{-3})$ corresponding to $\tau_o = 1$ is consistent with $N_e = 3 \times 10^{12}$ cm^{-3}. This implies that the mass of the absorbing cloud is of the order $M_b/M_\odot \sim 10^{-11}$.

7.4. Interpretation of the normalized He I 6678 line profile

Among the outstanding characteristics observed in the He I 6678 line of EW Lac normalized to the mean 1989 profile (Fig. 4) is the presence of weak emissions at nearly ± 400 km s^{-1} for which maximum intensities and positions vary only slightly, while the blue absorption "plateau" varies from a residual intensity 0.975 to about 0.998. Such behaviour is reminiscent of absorption lines produced by gaseous rings surrounding the star. It can be explained by preserving the source function factor $S \times \sum$(S = source function of the line; $\sum$ = projected surface of the ring) as the ring opacity decreases (Cidale & Ringuelet 1989). The high velocities at which the emission line shoulders appear in EW Lac imply that rings are rotating and perhaps expanding somewhat.

Another explanation for the He I 6678 line profile can be tried with a line source function perturbed by a variable chromosphere-corona like temperature structure of the stellar atmosphere. The observed intensity behaviour of the emission shoulders and the central "plateau" would demand, however, variable physical conditions in only those atmospheric layers which concern the central parts of the line profile, but these changes should keep the source function enhancement in the wings almost constant. Besides that, in this scenario the shoulder emissions are also signatures of the same variable stellar activity. In this paper we then explore the explanation for the line profiles shown in Fig. 4 based on circumstellar rings. Let us assume a central star surrounded by an inner cylindrical emitting ring at a distance $R_1 - R_e$ from the stellar surface (ring 1). The ring is assumed to have Keplerian rotational velocity $V_{\Omega 1}$, velocity V_{r1} in the radial direction, total height $2H_1$ and radial opacity $\tau_o^{(1)}$ at the center of the He I 6678 line. The emission produced by the ring was calculated assuming the presence of an underlying absorption photospheric component. The latter was obtained from a Gaussian profile with the same equivalent width as the 1989 mean profile, which was broadened by the adopted $V \sin i$ values. As no resulting "star + ring1" profile divided by the underlying stellar rotationally broadened profile was asymmetric enough to account for the narrower central component, we assumed the presence of a second ring (ring 2) situated at $R_2 > R_1$ and characterized by the set of parameters $V_{\Omega 2}$, V_{r2}, $2H_2$ and $\tau_o^{(2)}$. We assumed that both rings are symmetric with respect to the equatorial plane that contains the line of sight.

For typical electron densities in circumstellar envelopes of Be stars $10^{12} \leq N_e \leq 10^{13}$ cm^{-3} and at a temperature $T_e \sim 0.8 T_{\mathrm{eff}}$, the ratio of source terms in the source function of the He I 6678 line is $\epsilon B_\lambda(T_e)/\eta B_\lambda^* \simeq (15 \pm 7)(N_e/10^{12})$, where ϵB_λ = collisional source term and ηB_λ^* = radiative term, and the ratio of sink terms is $\epsilon/\eta \simeq (6 \pm 3)(N_e/10^{12})$, where ϵ = collisional sink term and η = radiative term. Hence, the source function of the line can be safely considered a collisionally dominated type. To a good degree of approximation the line source function can then be written (Mihalas 1978):

$$S(\tau_o) = \begin{cases} \epsilon^{1/2} B_\lambda(T_e) & \text{for } \tau_o \leq 1, \\ \epsilon^{1/2} B_\lambda(T_e) \tau_o^{1/2} & \text{for } \tau_o > 1. \end{cases} \quad (3)$$

For simplicity we adopted a Gaussian intrinsic line profile $\tau_\lambda = \tau_o e^{-(\Delta\lambda/\Delta\lambda_D)^2}$. The displacement$\Delta\lambda$ is produced by the total velocity along the line of sight $\pm\mu V_r \pm (1-\mu^2)^{1/2} V_\Omega$ [μ = cos(radial direction, line of sight)] and the signs are chosen according to the observed half of the ring and correspondence to its front or rear part.

For a non-negligible value of the source function and for a suitable opacity and $V_r = 0$, each ring produces a symmetric line profile with shoulder emissions and central absorption with a slight emission-like reversal. The "plateau" observed in the blue line velocity interval $-300 \leq V \leq -100$ km s^{-1} is obtained by introducing $V_{r1} \neq 0$, so that a P-Cyg like asymmetry is reproduced. However, the velocity in the radial direction needs to be $V1_{r1} \leq V_{\Omega 1}$, or else the blue emission component disappears. This condition, together with the high displacement of the emission shoulders, implies that the Keplerian velocity of the inner ring needs to be $V_{\Omega 1} \geq 400/\sqrt{2}$ km s^{-1}. At a given value of the source function of the inner ring, increasing values of τ_o produce increasing shoulder emissions but also a deeper central absorption "plateau". On the other hand, for a given opacity, increasing values of the source function increase the shoulder emission and reduce the "plateau" absorption.

At the low opacity "phases" the only way to obtain enough emission in the shoulders is by increasing the value of H. By trial and error we then obtained the ring parameters that roughly

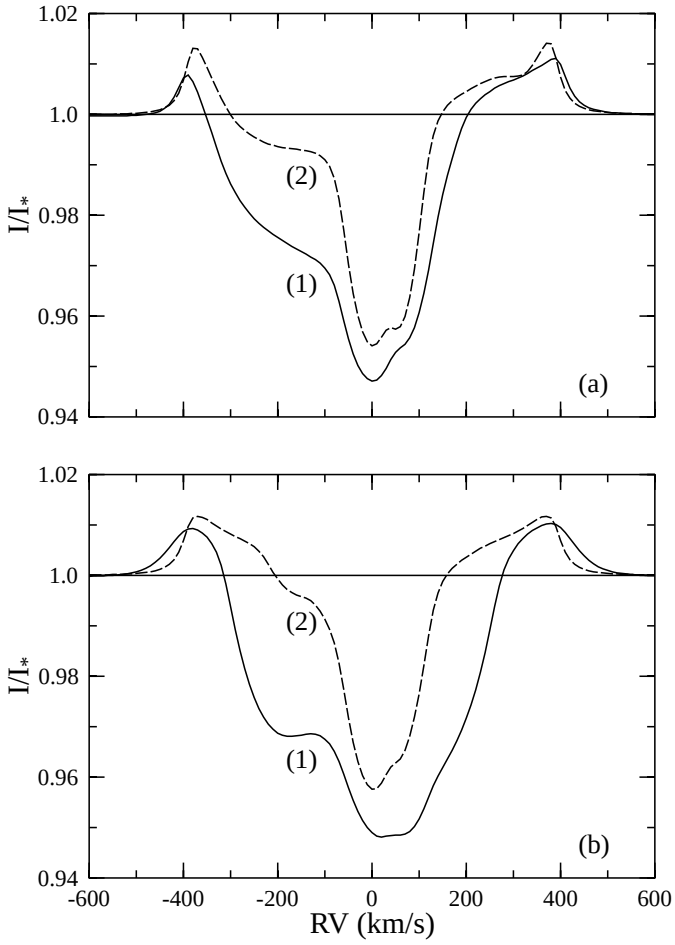

Fig. 18a and b. Model He I 6678 line profiles normalized to the photospheric component. Case **a** uses $V \sin i = 340\,\mathrm{km\,s^{-1}}$ and case **b** $V \sin i = 400\,\mathrm{km\,s^{-1}}$. Phase (1) is for higher $\tau_{\mathrm{o}}^{(1)}$ values and phase (2) for the lower ones (see Fig. 4)

account for the global features observed in the He I 6678 line shown in Fig. 4. Though the measured value of $V \sin i$ in EW Lac is $V \sin i = 340\,\mathrm{km\,s^{-1}}$, we calculated two sets of line profiles, one set for the measured $V \sin i$ (case a) and the other for $V \sin i = 400\,\mathrm{km\,s^{-1}}$ (case b). In each case we distinguish two "phases": "phase 1", which corresponds to a higher value of $\tau_{\mathrm{o}}^{(1)}$, and "phase 2" for a lower value of this opacity. The calculated line profiles which seem to resemble those observed closely are shown in Fig. 18. The corresponding model parameters are given in Table 8. Depending on the case, some observed features are better represented than others. At any rate, the crude necessarily model does not allow us to expect to account for all aspects observed. Some of them may be produced by radiation transfer effects due to density, temperature and velocity gradients in the rings, which were not taken into account in the present simulation.

However, from the results obtained we can draw some general conclusions. If the rings are due to ejected matter from the central star, the supposed Keplerian velocities cannot be caused simply by the angular momentum transfer from the stellar surface. This is, however, a general problem encountered in all models of circumstellar discs with Keplerian rotation. Within the uncertainties involved in the choice of ring parameters, the source function of each ring seems to be fairly constant: $S_1 = 0.12 \pm 0.03$ and $S_2 = 0.01 \pm 0.00$ as one passes from one opacity phase to the other. As the inner ring expands ($V_{\mathrm{r}1} < 0$), it seems to undergo acceleration, reduction of its radial opacity and increase of its height. The external ring is predominantly an absorption front ($S_2 \simeq 0.0$) situated at about the same distance whatever the opacity phase [$R_2 \simeq (3.0 \pm 0.2) R_\odot$]. Its velocity in the radial direction $V_{\mathrm{r}2} > 0$ implies a shrink phenomenon, and its opacity increases when the opacity of the inner ring decreases.

Table 8. Model parameters of circumstellar rings

Case	Ph	ring	V_{r} km s^{-1}	R/R_e	H/R_e	S/F_*	τ_{o}
a	1	1	−120	1.4	1.0	0.12	0.25
		2	+30	2.8	1.0	0.01	0.10
	2	1	−200	2.2	1.7	0.14	0.06
		2	+30	3.2	1.0	0.01	0.16
b	1	1	−30	1.5	1.0	0.08	0.45
		2	+30	3.0	1.0	0.01	0.04
	2	1	−80	2.5	1.7	0.14	0.05
		2	+30	3.0	1.0	0.01	0.12

Note: The source function is given in units of the stellar continuum flux F_* at λ 6678 Å. Ph=Phase.

As a matter of fact, it should be pointed out that components (a) and (b) (see Sect. 4.2) are seemingly produced in ring 1, and components (c) and (d) result from the absorbing effect of both rings.

We note that the expansion velocities needed to account for the shapes of line profiles do give only order of magnitudes and should not be considered as precise estimates. They do seem to be supersonic. The rings may then be the result of wind-circumstellar envelope interaction phenomena with shock fronts (Zorec et al. 2000), which need a more thorough description that cannot be done with the simple model used in the present calculation. Case b (Table 8) gives values more consistent with the time-scale of the components (a), (b) and V and R (see Sect. 4.2). However, these values are only indicative; the comparison remains limited as no reliable radial velocity value can be obtained without a good model for the pseudo-photosphere, which extends more or less in a radial direction and whose V_{rot} is a function of the radius.

8. Conclusions

The most important results presented in this study are:

- the finding that the underlying star is in fact a B1.5-B2 rapidly rotating main sequence object and the estimation of corresponding mass and radius
- the confirmation of multiperiodicity in line profile variations and the presence of the same periods (within the error bars)

in two sets obtained in very different conditions and at a 4-year interval. Many frequencies are commonly found in EW, FWHM, centroid RV, V and R emissions and lpv of He I 6678, and some of them are also present in Hα
- the beat phenomenon between the 1.39 and 1.55 c/d frequencies which is rather conspicuous in the RV of the He I centroid
- the linking of the four main detected frequencies to nrp. Possible solutions for frequencies 1.39, 2.76, 1.55 and 3.20 c/d indicate modes with $\ell \sim 2$–3 and $|m| \sim 2$–3
- the detection of pronounced minima in He I 6678 V emission with a period coherent with the stellar rotation period suggesting rotational modulation of CS material close to the star
- the evidence of signs of episodic matter outflows during the 1993 campaign such as a variable broad additional "pseudo-photospheric" component, discrete narrow blue-shifted absorptions and polarized flux enhancements
- the detection of blobs temporarily orbiting the star and giving rise to an expelled ring-like envelope
- the close correlation between continuum polarization and He I 6678 strength variations
- we also present an interpretation which reproduces the behaviour of the 1993 additional pseudo-photospheric contribution.

The pseudo-photosphere in EW Lac was found to be highly variable during the 8-day run in August-September 1993. It was probably the result of successive mass loss events by which matter is more or less continuously transferred to the envelope, and it seems that we observed at least one of these discrete events. We can imagine a rapid rotational acceleration of the upper photospheric layers and the expulsion of patchy blobs in the form of a ring-like structure with decreasing rotational speed. The different examples mentioned in Sect. 7.2 do support the formation of a rather cold, dense, rapidly rotating region between the "classical" photosphere and the envelope responsible for emission and shell lines. An important point is the close correlation between continuum polarization and He I 6678, which is expected from models, as the polarized flux comes from regions close to the photosphere (Poeckert & Marlborough 1979). The gradual mid-term increase of Hα can be explained both by the vanishing of the pseudo-photosphere and by some of the gas being added to the overall density of the line-forming region farther out. But the relation between Hα and polarization is not clear. Note that Sonneborn et al. (1988) found for ω Ori an increase in polarization rate correlated with brightness, but unrelated to Hα behaviour.

The description of He I 6678 line behaviour, considered in the context of circumstellar rings, may actually reveal the presence of phenomena related to circumstellar envelope building mechanisms. In fact, the expansion velocities needed to account for the shapes of line profiles are supersonic. The rings may then represent shock fronts due to wind-circumstellar envelope interaction phenomena. These shock fronts are in particular expected in the ablation process of parcels of matter ejected by the stellar wind. The mechanism leads to a mass-loaded flow which can be considered as embodying the circumstellar envelope of the Be star (Zorec et al. 2000).

As EW Lac is not among the brighter Be stars, spectroscopic monitoring was restricted in 1989 and 1993 to one of the strongest He I lines, due to the limited available wavelength range with current instrumentation. He I 6678 has been revealed as very sensitive to the formation and development of a pseudo-photosphere related to discrete mass loss events; consequently it is not suitable for the search for non-radial pulsations, though multiperiodicity in the line profile was nicely confirmed. Newly operating, more sensitive echelle spectrographs will enable us to extend the investigation of nrp and stellar activity by observing many lines formed at different depths of the photosphere and to obtain a better image of atmospheric phenomena in this star.

Acknowledgements. We wish to thank A. Garcia for help in the drawing of figures and A. Mekkas for technical assistance. We are grateful to the anonymous referee for a critical reading of the manuscript and constructive comments. This research has made use of the services of the Centre de Données Stellaires, Strasbourg, France. Special thanks to Judy Coughlin for a most valuable discussion.

References

Balona L.A., Rozowsky G., 1991, MNRAS 251, 668
Cidale L.S., Ringuelet A.E., 1989, PASP 101, 417
Castor J.I., Smith L.F., van Blerkom D., 1970, ApJ 159, L1119
Collins II G. W., Sonneborn G.H., 1977, ApJ 34, 41
Collins II G.W., Truax R.J., Cranmer S.R., 1991, ApJS 77, 541
Divan L., Zorec J., 1982, In: Perryman M.A.C., Guyenne T.D. (eds.) The Scientific Aspects of the Hipparcos Space Astrometric Mission. ESA-SP 177, p. 101
Floquet M., Hubert A.M., Janot-Pacheco E., et al., 1992, A&A 264, 177
Floquet M., Hubert A.M., Hubert H., et al., 1996, A&A 310, 849
Gies D.R., Kullavanijaya A., 1988, ApJ 326, 813
Gies D.R., 1994, In: Balona L.A., Henrichs H.F., Le Contel J.M. (eds.) Pulsation, Rotation and Mass Loss in Early-type Stars. IAU Symp. 162, p. 89
Hanuschik R.W., Hummel W., Sutorius E., et al., 1996, A&AS 116, 309
Harmanec P., 1983, Hvar Obs. Bull. 7, 55
Hirata R., 1993, Be Star Newsletter 31, 20
Hirata R., 1995, PASJ 47, 195
Hubeny I., 1988, Computer Physics Comm. 52, 103
Hubeny I., Lanz T., Jeffery C.S., 1994, In: Jeffery C.S. (ed.) Newsletter on Analysis of Astronomical Spectra No. 20, St Andrew Univ., p. 30
Hubert A.M., Floquet M., Hao J.X., et al., 1997, A&A 324, 929
Hubert A.M., Floquet M., 1998, A&A 335, 565
Janot-Pacheco E., Jankov S., Leister N.V., et al., 1999, A&AS 137, 407
Kambe E., Ando H., Hirata R., 1993, A&A 273, 435
Koubský P., Harmanec P., Kubat J., et al., 1997, A&A 328, 551
Lester D.F., 1975, PASP 87, 177
Maeder A., Meynet G., 1988, A&AS 76, 411
Mathias P., Waelkens C., 1995, A&A 300, 200
Mihalas D., 1978, Stellar Atmospheres. Freeman
Moujtahid A., Zorec J., Hubert A.M. et al., 1999, A&A 349, 151

Moujtahid A., Zorec J., 2000, In: Smith M., Henrichs H., Fabregat J. (eds.) The Be Phenomenon in Early-Type Stars. IAU Coll. 175 (in press)
Moujtahid A., Zorec J., Hubert A.M., 2000, In: Smith M., Henrichs H. Fabregat J. (eds.) The Be Phenomenon in Early-Type Stars. IAU Coll. 175 (in press)
Okazaki A.T., 1996, PASJ 48, 305
Pavlovski K., 1987, Ap&SS 134, 317
Pavlovski K., Schneider H., 1990, A&A 228, 361
Pavlovski K., Ružić Ž., Pavlović M., et al., 1993, Ap&SS 200, 201
Pavlovski K., Harmanec P., Božić H., et al., 1997, A&AS 125, 75
Percy J.R., Desjardins A., Yeung D., 1996, JAAVSO 25, 14
Peters G.J., 1998, In: Kaper L., Fullerton A.W. (eds.) Cyclical Variability in Stellar Winds. ESO Astrophysics Symp., Springer, p. 127
Peters G.J., Gies D.R., 2000. In: Smith M., Henrichs H., Fabregat J. (eds.) The Be Phenomenon in Early-Type Stars. IAU Coll. 175 (in press)
Poeckert R., Bastien P., Landstreet J.D., 1979, AJ 84, 812
Poeckert R., Marlborough J.M., 1979, ApJ 233, 259
Rivinius Th., Baade D., Štefl S., et al., 1998a, A&A 333, 125
Rivinius Th., Baade D., Štefl S., et al., 1998b, A&A 336, 177
Schrijvers C., Telting J.H., Aerts C., et al., 1997, A&AS 121, 343
Schrijvers C., Telting J.H., 1999, A&A 342, 453
Slettebak A., Collins II G.W., Truax R.J., 1992, ApJS 81, 335
Slettebak A., Kuzma T.J., Collins II G.W., 1980, ApJ 242, 171
Smith M., Polidan R.S., 1993, ApJ 408, 323
Smith M., Hubeny I., Lanz T., 1994, In: Balona L.A., Henrichs H.F., Le Contel J.M. (eds.) Pulsation, Rotation and Mass Loss in Early-type Stars. IAU Symp. 162, p. 273
Sonneborn G., Grady C.A., Wu Chi-Chao, et al., 1988, ApJ 325, 784
Stagg C.R., Božič H., Fullerton A., et al., 1988, MNRAS 234, 1021
Štefl S., Aerts C., Balona L.A., 1999, MNRAS 305, 505
Telting J.H., Schrijvers C., 1997, A&A 317, 723
Townsend R.H.D., 1997a, Ph.D. Thesis, University College London
Townsend R.H.D., 1997b, MNRAS 284, 839
Zorec J., 1986, Thèse d'Etat, Université de Paris VII
Zorec J., Briot D. 1997, A&A 318, 443
Zorec J., Hubert A.M., Moujtahid A. 2000. In: Smith M., Henrichs H. and Fabregat J. (eds.) The Be Phenomenon in Early-Type Stars. IAU Coll. 175 (in press)